Chapter 4

In vitro Investigations on Effect of Ponatinib on interplay between Autophagy and Apoptosis Focusing upon Beclin-1 and Bcl-2 Interaction *

Abstract

The interplay between Beclin-1 and Bcl-2 is crucial in controlling two vital processes in cells: autophagy and apoptosis. Autophagy helps cells survive during times of stress or damage, while apoptosis leads to cell death. Bcl-2 typically hinders autophagy by interacting with Beclin-1. However, disrupting this interaction can shift the balance towards autophagy or apoptosis, depending on the situation. In a previous study, we found that Ponatinib, a tyrosine kinase inhibitor, to effectively bind to the interface between Beclin-1 and Bcl-2, thereby interfering with the interaction between Beclin-1 and Bcl-2. This led us to investigate how Ponatinib affects autophagy and apoptosis in MCF-7 cells, a type of breast cancer cell. Our computational data reported in earlier chapter together with experimental data reported in the current chapter suggests that Ponatinib disrupts the interaction between Beclin-1 and Bcl-2. The disruption of interaction is reflected through shift from autophagy to apoptosis in these cells as seen using various markers of autophagy and apoptosis which indeed depends on how long the cells are exposed to the drug. Ponatinib along with Rapamycin shows synergistic effect and triggers the autophagy-mediated cell death. Initially, the level of autophagy is upregulated and with due course of time, there is inhibition of autophagic flux and subsequently, this inhibition triggers apoptosis. It is important to note that apoptosis is a pathway that leads to cell death and can be beneficial in clearing out cancer cells. In summary, our computational and experimental data provide insights into how Ponatinib may be effective in treating cancer by influencing the interaction between Beclin-1 and Bcl-2.

*Part of the work is prepared for communication.

4.1 Introduction to the interplay between Autophagy and Apoptosis

In the presence of favourable environmental conditions, cells endeavour to maintain a delicate equilibrium between anabolic and catabolic processes while facilitating the recycling of cellular components (Kim and Lee 2014). One pivotal regulatory mechanism crucial for preserving this equilibrium is autophagy, a catabolic pathway involving the sequestration of long-lived proteins and damaged organelles into double-membrane vesicles known as autophagosomes. These autophagosomes are subsequently delivered to lysosomes, where the enclosed material is degraded and recycled. Furthermore, cellular stressors can induce cell death; apoptosis, a programmed cell death process, serves as a central regulatory mechanism. Apoptosis can be triggered either through the extrinsic pathway, involving death receptor activation, or the intrinsic pathway, marked by the release of mitochondrial death-promoting factors, such as cytochrome c (cyt c). The Cyt c activation ultimately activates caspases, leading to characteristic biochemical and morphological changes such as chromatin condensation, DNA fragmentation, cell shrinkage, and membrane blebbing (CW and SH 2018).

Although apoptosis is recognized as the primary mechanism of cell death, the functional role of autophagy in cell survival and cell death remains a subject of intense debate. Autophagy exhibits dual functionality, as it can either promote or counteract cell death signaling depending on the cellular milieu, cell types, and stimuli. A complex interplay between autophagy and apoptosis is believed to exist, and as a result, the molecular interactions and functional relationships between these two pathways have garnered significant attention.

The regulation of autophagy relies on a set of evolutionarily conserved genes, collectively referred to as atg (autophagy-related genes). One key participant in this pathway

is Bcl-2 interacting protein 1 (Beclin-1), which serves as the mammalian ortholog of yeast Atg6/Vps30. Beclin-1 was initially identified through a yeast-two hybrid assay as a protein interacting with Bcl-2. It is worth noting that Beclin-1 operates as a haploinsufficient tumor suppressor gene and is often monoallelically deleted in various human sporadic cancers, including breast, ovarian, and prostate cancer. Such deletions lead to a downregulation of autophagy in these cancer types. Beclin-1 plays a pivotal role by interacting with multiple proteins from both autophagic and apoptotic pathways. Among its domains, the BH3 domain facilitates interaction with the anti-apoptotic protein Bcl-2. Normally, the binding of Bcl-2 to Beclin-1 inhibits autophagy. However, as cellular stress escalates, this interaction weakens, initially resulting in upregulated autophagy. Subsequently, as stress intensifies, Beclin-1 is dissociated from Bcl-2, leading to a significant upregulation of autophagy. This heightened autophagic activity triggers the activation of various signaling molecules, ultimately culminating in apoptosis (Abedin *et al.* 2006). This intricate interplay between Beclin-1 and Bcl-2 interactions underscores their potential role in the convergence of autophagy and apoptotic cell death, thereby regulating a wide range of physiological and pathophysiological conditions (Wei *et al.* 2008a).

To elucidate the fate and functional dynamics of autophagic proteins during the early stages of apoptosis, our research has been predominantly centered on examining the intricate interplay between Beclin-1 and Bcl-2. We have previously elucidated a putative binding affinity between the pharmaceutical agent Ponatinib and the BH3 domain of Beclin-1 through our *in silico* work (Prerna and Dubey 2021). Consequently, the current study endeavours to validate these computational findings through *in vitro* experimentation. Our specific objective is to employ Ponatinib as an agent to disrupt the Beclin-1-Bcl-2 interaction, thereby facilitating autophagy-mediated cell death in breast cancer cells.

Ponatinib, categorized as a third-generation tyrosine kinase inhibitor (TKi), has demonstrated significant therapeutic enhancements for the adult cohort diagnosed with chronic myeloid leukemia (CML). The multifaceted mechanisms underlying Ponatinib's therapeutic efficacy involve intricate regulatory control over an array of intracellular signaling pathways, notably including STAT3, PI3K/AKT, and ERK. These pathways function as pivotal facilitators of tumor cell proliferation and survival. Nonetheless, the emergence of resistance to Ponatinib, as evidenced both in preclinical and clinical settings, has prompted the imperative for comprehensive elucidation of the underlying basis of acquired resistance to this therapeutic intervention. In recent years, autophagy has emerged as a consequential cytoprotective mechanism triggered in response to various chemotherapeutic agents. A substantial body of research underscores the critical role of autophagy in conferring survival advantages to cancer cells following exposure to anti-neoplastic agents. Notably, a spectrum of tumor cell types, when subjected to tyrosine kinase inhibitors, activates the autophagic machinery in response to chemical insults, thereby mitigating cellular stress. This adaptive response has been observed as a salient feature in breast cancer cells as well.

In the scope of this study, our primary aim was to elucidate the intricate cross-talk among distinct signaling pathways and unravel the fate of the proteins Beclin-1 and Bcl-2 within this intricate interplay. To achieve this, we conducted a comprehensive examination of the potential for autophagy-driven cell death in breast cancer cells when exposed to Ponatinib (PON). Employing an *in vitro* approach, we systematically explored the synergistic interactions between PON and a range of modulators influencing autophagy and apoptosis. Our findings notably underscore the pronounced effectiveness of these combined treatments in significantly impeding the survival of breast cells.

4.2 Materials and Methods

4.2.1 Reagents and antibodies: All compounds, including Ponatinib, HY-12047; Rapamycin, HY-10219; 3-MethylAdenine, HY-19312; and SP600125, HY-12041, which were employed in this investigation, were acquired from MedChemExpress. These compounds were dissolved according to the recommended solvent protocols provided by the supplier's website. Doxorubicin, a pharmaceutical agent used in this study, was procured from Sigma (catalog number D1515). The compounds were solubilized in accordance with the recommended solvent protocols specified by the respective suppliers on their websites. The master stock solutions of these drugs were meticulously stored at -20°C, and the working solutions were freshly prepared immediately prior to each experimental procedure. The antibodies utilized in this research are itemized as follows: Anti-Beclin-1 (obtained from Cell Signaling Technology, catalog number 3738), Anti-phospho-Bcl-2 (from Cell Signaling Technology, catalog number 2827), Anti-Bcl-2 (purchased from Santa Cruz, catalog number 7382), Anti-β-Actin (sourced from Invitrogen, catalog number AM4302), Anti-rabbit IgG, HRP-linked antibody (acquired from Cell Signaling Technology, catalog number 7074), Anti-mouse IgG, HRP-linked antibody (sourced from Invitrogen, catalog number 62-6520), Alexa Fluor 555 (from Invitrogen, catalog number A21422), and Alexa Fluor 633 (from Invitrogen, catalog number A21071). For specific assays, the cell apoptosis kit (catalog number 640930) was procured from BioLegend, and the CYTO-ID autophagy detection kit (catalog number ENZ-51031) was sourced from Enzo Life Sciences. The cDNA kit was purchased from Thermo Scientific (catalog number K1621).

4.2.2 Cell line and the Culture conditions: Human breast cancer cells (MCF-7) were procured from the National Centre for Cell Science (NCCS) in Pune, India. The cells were cultivated in Dulbecco's Modified Eagle Medium (DMEM) culture medium (Gibco, catalog number 11995-065), enriched with 10% Fetal Bovine Serum (FBS) (Gibco, catalog number

10270106), and 1% Penicillin-Streptomycin (Pen-Strep) antibiotic solution (Himedia, catalog number A018). The cell cultures were maintained at a controlled environment of 37°C with 5% CO2 in a humidified incubator.

To investigate the impact of Ponatinib (PON) on these cells, they were exposed to PON for durations as specified and at doses indicated for each experiment. In the context of combinatorial studies, various modulators affecting autophagy and apoptosis were introduced one hour prior to the administration of PON. To assess the effect of these modulators over Ponatinib, the cells were treated with following working concentrations: Rapamycin, 20 nM; 3-Methyladenine, 5 mM; Doxorubicin, 4 μM; and SP600125, 10 μM.

4.2.3 Metabolic activity assay: To determine the inhibitory concentration (IC50) of Ponatinib (PON), representing the concentration at which the drug induces a 50% reduction in cell viability, the following experimental procedure was employed. An initial seeding of ~$6x10^3$ cells was seeded in each well of a 96-well plate, ensuring that the cells were in the exponential growth phase. Subsequently, after a 24-hour incubation period, the culture medium was replaced with fresh medium, and PON was administered. The treatment was executed over a 24-hour timeframe. Cell viability assessments were carried out at the specified time point by evaluating metabolic activity via the utilization of the Thiazolyl Blue Tetrazolium Bromide (MTT) reagent, obtained from Sigma-Aldrich (catalog number M5655). The results were compared with those from control cells treated with an equivalent amount of dimethyl sulfoxide (DMSO).

For a detailed method, following overnight confluency, the cells were treated with PON, which was serially diluted in the culture medium. After 24 hours of treatment, the culture medium was aspirated, and 50 μL of MTT solution (5 mg/mL in PBS) was added to each well. The cells were then incubated for 4 hours at 37°C. Following the incubation period, the MTT solution was removed, and the resulting formazan crystals were dissolved in

200 µL of dimethyl sulfoxide (DMSO). Subsequently, absorbance readings were taken at 540 nm using a BioTek microplate reader. The IC50 value was calculated using GraphPad Prism software. Each experiment was performed in triplicate and performed at least two separate times to ensure the reliability of the results.

4.2.4 RNA extraction and cDNA synthesis: A total of ~$1x10^5$ cells were seeded into each well of a 6-well plate. After allowing the cells to adhere overnight, treatments with Ponatinib (PON) or various combinations of drugs were initiated, with incubation periods of 24 and 48 hours. Subsequent to these indicated time points, total RNA extraction was carried out using TriZol reagent (Invitrogen, catalog number 15596026), following the guidelines provided in the instruction manual. The integrity of the isolated RNA was confirmed through 1.8% agarose gel electrophoresis, and its concentration was determined by measuring the optical density (OD) at 260 nm using a NanoDrop spectrophotometer. The RNA samples were used to generate complementary DNA (cDNA) in accordance with the protocols outlined in the cDNA kit manual. The resulting cDNA was stored at -20°C for subsequent analysis.

These cDNA samples were subsequently employed for quantifying the relative mRNA expression levels of selected genes. The primer sequences for all targeted genes were sourced from the NCBI database and were generated by Integrated DNA Technologies (IDT). The primer sequences are presented in the accompanying table.

4.2.5 Real-time PCR (qPCR) analysis: To quantify the expression of each target gene, SYBR Green master mix (Applied Biosystems) was employed, utilizing 10 ng of cDNA per reaction. Real-time quantitative polymerase chain reaction (qPCR) was conducted using an Applied Biosystems instrument. The target genes used in this study were Beclin-1, Bcl-2, Cytochrome c and GAPDH. There primers for these genes were synthesized by Eurofins, Varanasi, India. The list of the primers is mentioned below. The thermal cycling parameters

were as follows: an initial denaturation at 95°C for 10 minutes, followed by 40 cycles of amplification at 95°C for 15 seconds and 60°C for 1 minute. A melting curve analysis was performed at 60°C for 15 seconds to confirm the specificity of the amplification. The acquired data were subjected to a dual normalization process. First, the data were normalized to the untreated control samples, and subsequently, they were normalized to the expression levels of the reference gene, GAPDH. The ΔΔCT (delta-delta threshold cycle) values were subsequently calculated employing GraphPad Prism software.

Name	Sequence
Hs_BECN1_FP	5′-TGTCACCATCCAGGAACTCA-3′
Hs_BECN1_RP	5′-CTGTTGGCACTTTCTGTGGA-3′
Hs_Bcl2_FP	5′-TTGTGGCCTTCTTTGAGTTCGGTG-3′
Hs_Bcl2_RP	5′-GGTGCCGGTTCAGGTACTCAGTCA-3′
Hs_CytochromeC_FP	5’-GAGGCAAGCATAAGACTGGA-3’
Hs_CytochromeC_RP	5’-TACTCCATCAGGGTATCCTC-3’
Hs_GAPDH_FP	5′-GAAATCCCATCACCATCTTCCAGG-3′
Hs_GAPDH_RP	5′-GAGCCCCAGCCTTCTCCATG-3’

4.2.6 Western blot assay: A total of ~$1x10^5$ cells were seeded into each well of a 6-well plate. Subsequent to the treatment period, the culture medium was removed, and the cells were gently rinsed with ice-cold phosphate-buffered saline (PBS). Following this, the cells were lysed with ice-cold RIPA buffer (Sigma, catalog number R0278) by gentle scraping with a cell scraper. The cell lysate was then collected, and centrifugation was performed at 12,000 rpm for 30 minutes at 4°C. The resulting supernatant was carefully aspirated into a fresh tube, and the protein concentration was quantified utilizing the BCA protein assay kit (Invitrogen, catalog number 23225). Equal quantities of proteins (40 μg) were resolved via

12% SDS-Polyacrylamide gel electrophoresis and subsequently transferred onto a pre-wetted PVDF membrane (Macherey-Nagel, catalog number 741260). The transfer was accomplished using a semi-dry blotter at 300 mA for 30 minutes. The PVDF membrane was then subjected to blocking with either 5% Bovine Serum Albumin (BSA) or non-fat dry milk in Tris-Buffered Saline with Tween 20 (TBST) buffer (comprising 25 mM Tris, 150 mM NaCl, and 0.1% Tween-20, pH 7.6) for a duration of 2 hours at room temperature. Subsequently, the membrane was incubated with primary antibodies (Anti-Beclin-1, 1:1000; Anti-phospho-Bcl-2, 1:500; Anti-Bcl-2, 1:200; Anti-β-Actin, 1:5000) in the blocking buffer, overnight at 4°C under gentle agitation condition. After incubation, the membranes were washed with TBST buffer to remove unbound antibodies and were subsequently incubated with Horseradish Peroxidase (HRP)-conjugated secondary antibodies (Anti-rabbit IgG, HRP-linked antibody, 1:3000; Anti-mouse IgG, HRP-linked antibody, 1:10000) for 2 hours at room temperature. Excess antibodies were removed by further washing with TBST. Finally, the protein bands were visualized by employing an ECL-detecting reagent (Invitrogen, catalog number WP20005) and captured using a ChemiDoc imaging system (Bio-Rad Laboratories). The intensity of the bands was quantified and analyzed via densitometric analysis using ImageJ software. All the data is expressed as the fold change relative to the control sample.

4.2.7 Immunofluorescence assay: Immunofluorescence analyses were conducted to facilitate the visualization and detection of various cellular components and proteins. Specifically, autophagosomes were visualized using the CYTO-ID autophagy detection kit, while the proteins Beclin-1 and Bcl-2 were detected through the application of Anti-Beclin-1 (diluted at 1:100) and Anti-Bcl-2 (diluted at 1:50) antibodies. A total of ~$5x10^3$ cells were seeded into each well of a 6-well plate having coverslip into it. Following the treatment, the cultured cells, which were grown on coverslips, underwent a series of meticulous steps. Initially, they were gently washed with 1X assay buffer (as provided in the kit) to ensure

secure adherence to the coverslip. Subsequently, the coverslip was inverted and placed on a parafilm, onto which 25 μL of Microscopy dual detection reagent (included in the kit) was dispensed. This assembly was then incubated at 37°C for a duration of 30 minutes, all while being shielded from light. The cells were subsequently subjected to a gentle wash with 1X assay buffer and then underwent fixation with ice-cold 4% (w/v) paraformaldehyde in phosphate-buffered saline (PBS) at room temperature (RT) for 20 minutes. Following fixation, the cells were washed with ice-cold PBS and subsequently subjected to permeabilization using 0.5% (v/v) Triton X-100 in PBS for 10 minutes at RT. After this permeabilization step, the cells were again washed with PBS. To minimize non-specific binding and interactions, the cells then underwent a blocking procedure, during which they were treated with a blocking solution composed of 3% fetal bovine serum (FBS) (v/v) in PBS for 30 minutes. This was followed by a replacement of the blocking buffer with primary antibodies, suitably diluted in the blocking buffer. The cells were then incubated for a period of 2 hours at RT. Subsequent to primary antibody incubation, the cells were washed with PBS and further subjected to incubation with secondary antibodies, labeled with fluorescent dyes such as Alexa Fluor 555 (1:200) and Alexa Fluor 633 (1:200). This secondary antibody incubation was conducted in the blocking buffer for a duration of 45 minutes at RT. Following this, the cells underwent an additional wash with PBS. The coverslip, now carrying the fluorescently labeled cells, was mounted over a glass slide using an appropriate mounting medium, and the edges of the coverslip were securely sealed with biologically compatible nail polish. Subsequently, the stained cells were imaged using a Zeiss LSM 800 confocal microscope, capturing images at a 60X magnification. The acquired images were then subjected to analysis using ImageJ software for further data extraction and quantification.

4.2.8 Apoptosis Assay: A total of ~1-2x10^5 cells were seeded into each well of a 6-well plate. The paragraph describes an experiment aimed at assessing the impact of Ponatinib (PON) in conjunction with other modulators of autophagy and apoptosis on breast cancer cells. The cell apoptosis assay involved quantifying phosphatidylserine levels within the cells by employing APC Annexin V and 7-AAD dyes for staining. The experimental protocol was meticulously adhered to, following the manufacturer's guidelines. Subsequently, the samples were expeditiously acquired within one hour using a flow cytometer (CytoFlex). The dot plot generated post-acquisition was subjected to analysis through FCS Express software, which facilitated the identification of distinct cell populations. These included the live cell population located in the lower left quadrant, the early apoptotic population in the lower right quadrant, the late apoptotic population in the upper right quadrant, and the necrotic population in the upper left quadrant. Each sample yielded 100000 recorded events. This comprehensive experiment was executed at both 24-hour and 48-hour time points and was conducted in duplicate for enhanced rigor and reliability.

4.2.9 Statistical analysis: The data was derived from a total of three distinct, independent experiments. The resulting data were then presented as the mean value ± standard error of the mean (SEM). All statistical analyses and the graphical representation of the data were undertaken using GraphPad Prism 5 software.

4.3 Results and Discussion

4.3.1 Ponatinib inhibited the proliferation of human breast cancer cells MCF-7.

In a significant portion of breast cancer cells, monoallelic deletion of the *beclin-1* gene results in downregulation of the Beclin-1 protein, leading to a subsequent decrease in autophagy levels. The rationale behind this study is the potential therapeutic benefit of upregulating the autophagic process as a means to clear tumor. Our previous computational research had identified Ponatinib as a candidate drug that could potentially bind to Beclin-1's surface and disrupt its interaction with Bcl-2, a pivotal step in regulating autophagy. To validate these *in silico* findings, comprehensive *in vitro* experiments were conducted, utilizing MCF-7 breast cancer cells as the experimental model.

The primary objective was to assess the impact of Ponatinib (PON) on the viability of MCF-7 cells was assessed through the utilization of the MTT assay. As depicted in the figure 4.1, PON exhibited a dose-dependent reduction in cell viability across a range of concentrations, spanning from 50 μM down to 0.04 μM. At the 24-hour time point, the half-maximal inhibitory concentration (IC50) was calculated and determined to be approximately 2.44 μM. This particular concentration was subsequently employed for the treatment of MCF-7 cells in subsequent experiments.

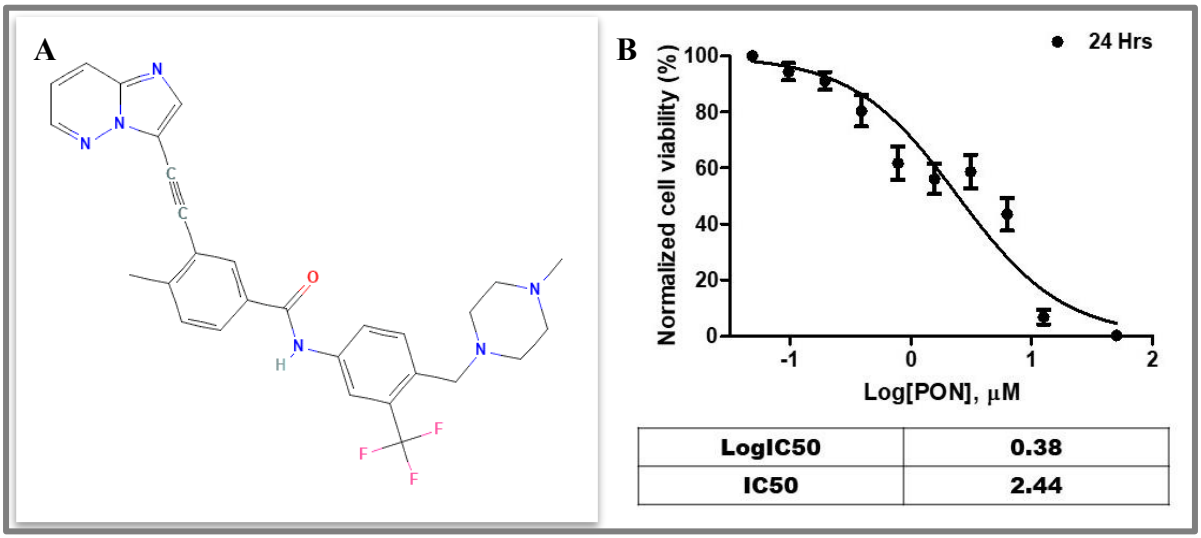

Figure 4.1. PON reduces the cell viability in MCF-7 cells. (**A)** The chemical structure of Ponatinib (PON) is depicted for reference. (**B)** The effect of PON was meticulously assessed on the human breast cancer cell line, MCF-7, via the implementation of the MTT Assay. The cells were subjected to pre-treatment with PON in a systematic serial dilution scheme, commencing with the highest concentration of 50 µM. The concentration of 2.4 µM was identified as the inhibitory concentration of PON, capable of reducing cell viability by approximately 50%. The presented data has been normalized with respect to the control sample, denoting 100% viability. The symbols and bars within the figure illustrate the mean values accompanied by the standard error of the mean (SEM) derived from three distinct and independent experimental repetitions.

4.3.2 Ponatinib induces the autophagy initially, further inhibits the autophagic flux, and subsequently triggers apoptosis in MCF-7 cells.

The objective was to determine if Ponatinib, when applied at different concentrations (IC50 and 2IC50), could indeed regulate the Beclin-1 and Bcl-2 interaction. This regulation was anticipated to initially upregulate autophagy, which was examined in various ways. To evaluate the impact of Ponatinib on the interaction between Beclin-1 and Bcl-2, we conducted comprehensive assessments at both the RNA and protein levels. At the RNA level, we utilized several key markers, including Beclin-1, Bcl-2, and cytochrome-c. In this analysis, we employed GAPDH as a loading control. The influence of Ponatinib was investigated in the presence of various pharmacological agents known to regulate autophagy and apoptosis, such as Rapamycin (Rap), 3-Methyladenine (3-MA), Doxorubicin (Dox), and SP600125. Furthermore, we examined the effect of Ponatinib on the regulation of the Beclin-1-Bcl-2 interaction at the protein level using Western blot assays (Representative images are depicted in Figure 4.2). This protein-level analysis encompassed the assessment of key proteins, including Beclin-1, Bcl-2, and phospho-Bcl-2. β-Actin served as the loading control for this experiment. The entire analysis was conducted at two distinct time points, 24 and 48 hours. Additionally, we validated the impact of Ponatinib on the Beclin-1-Bcl-2 interaction using immunofluorescence assays (Representative images are shown in Figures 4.3 to 4.7). In this context, we assessed Ponatinib's effect by staining autophagic vacuoles formed during the autophagy process. We also examined the levels of Beclin-1 and Bcl-2 proteins using antibodies specific to these targets. Following the assessment of Ponatinib's effects through a series of experiments, we simplified the representation of the data using densitometric methods. This data was then presented in the form of bar diagrams for enhanced visualization and clarity.

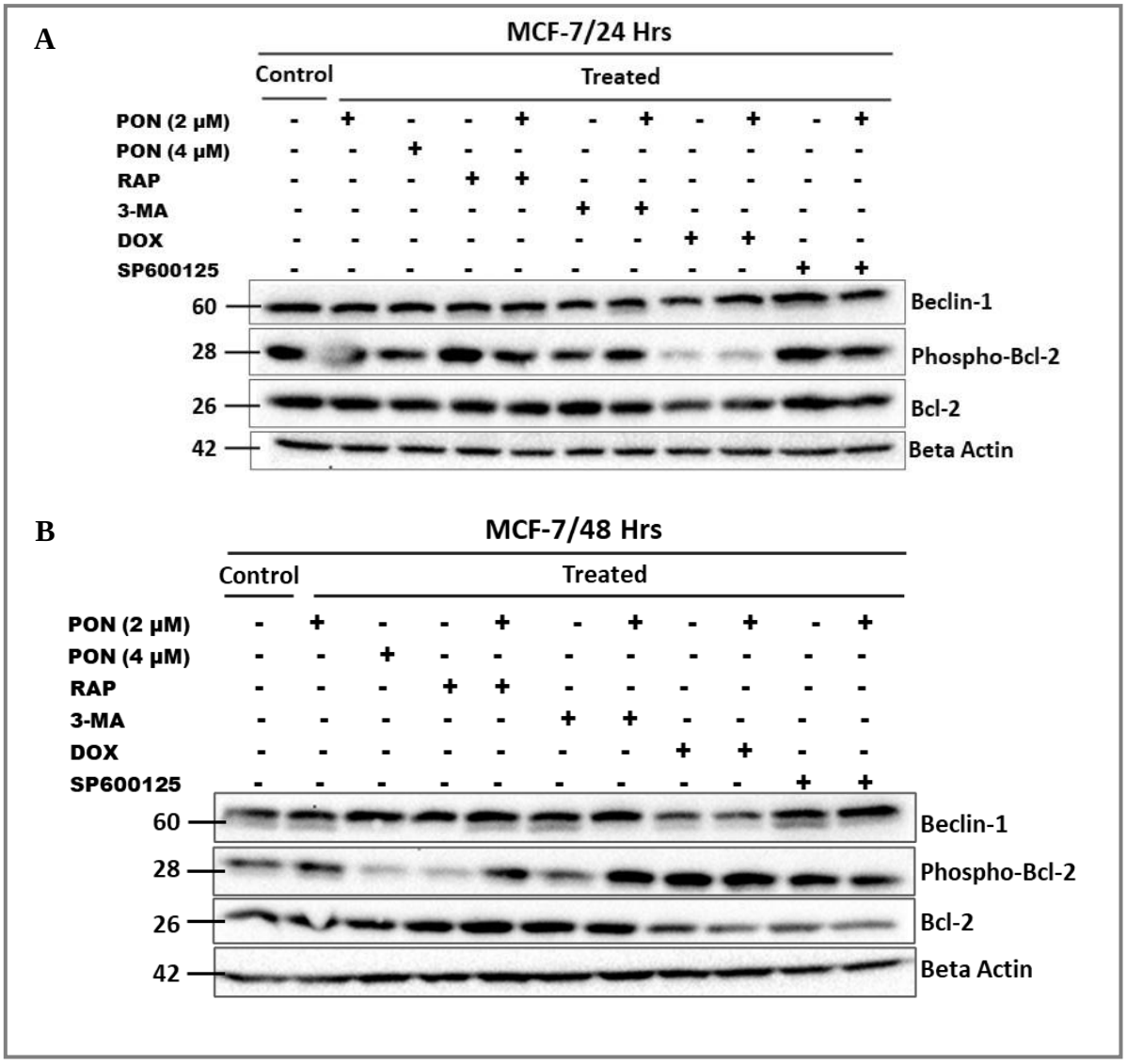

Figure 4.2. Representative image showing the impact of several regulators of autophagy and apoptosis with or without the addition of Ponatinib on Autophagy and Apoptosis Markers using western blot analysis. The western blot analysis presents representative images depicting the probing of total cellular proteins with markers pertaining to the regulatory pathways of autophagy and apoptosis. This image illustrates the influence of several regulators of autophagy and apoptosis with or without the addition of Ponatinib on Beclin-1, Bcl-2, and phospho-Bcl-2 levels in MCF-7 cells, with the molecular weight of each protein indicated in kilodaltons (KDa). These assessments were conducted in the presence or absence of autophagic and apoptotic regulators and extended over 24 hours **(A)** and 48 hours **(B)**. β-Actin immunoblotting was implemented as a loading control to ensure consistency. Notably, the displayed results are representative of three separate and independent experiments, with untreated cells serving as the control.

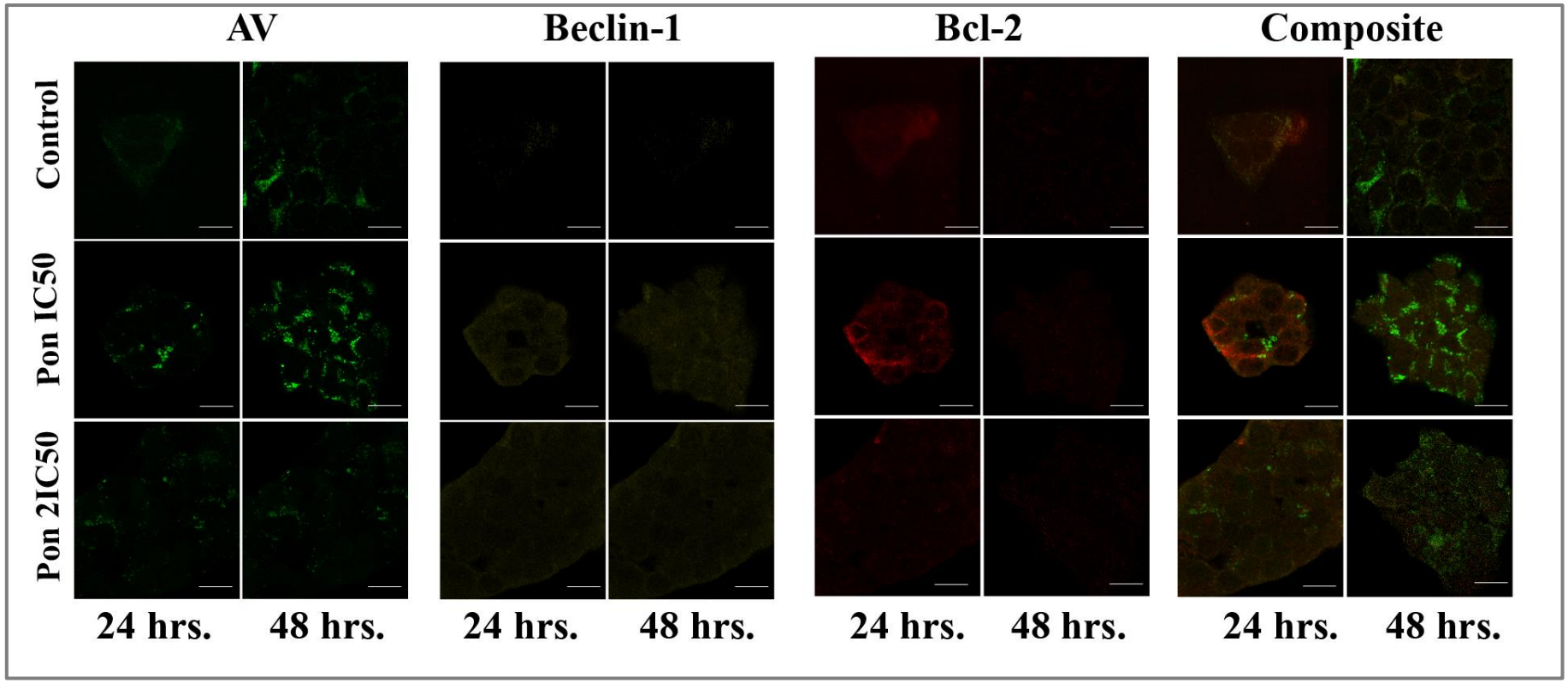

Figure 4.3. Representative images of immunofluorescence of Beclin-1, Bcl-2 and autophagic vacuoles in the presence of Ponatinib (Pon). The provided figures illustrate representative immunofluorescence images showcasing the staining of Beclin-1 and Bcl-2 in MCF-7 cells subjected to PON treatment at IC50 and 2IC50 concentrations, across 24 and 48-hour time points. These images also incorporate the visualization of autophagic vacuoles, distinguished by their labeling with CYTO-ID Autophagic vacuole detecting reagent, presented in a green colour. The fluorescence intensity data were meticulously quantified and graphically represented using GraphPad Prism software, with the detailed graphical representation being presented separately. Furthermore, the analysis of these images was carried out utilizing ImageJ software. The images were acquired under a substantial magnification level of x600, with a scale bar indicating a measurement of 20 μm.

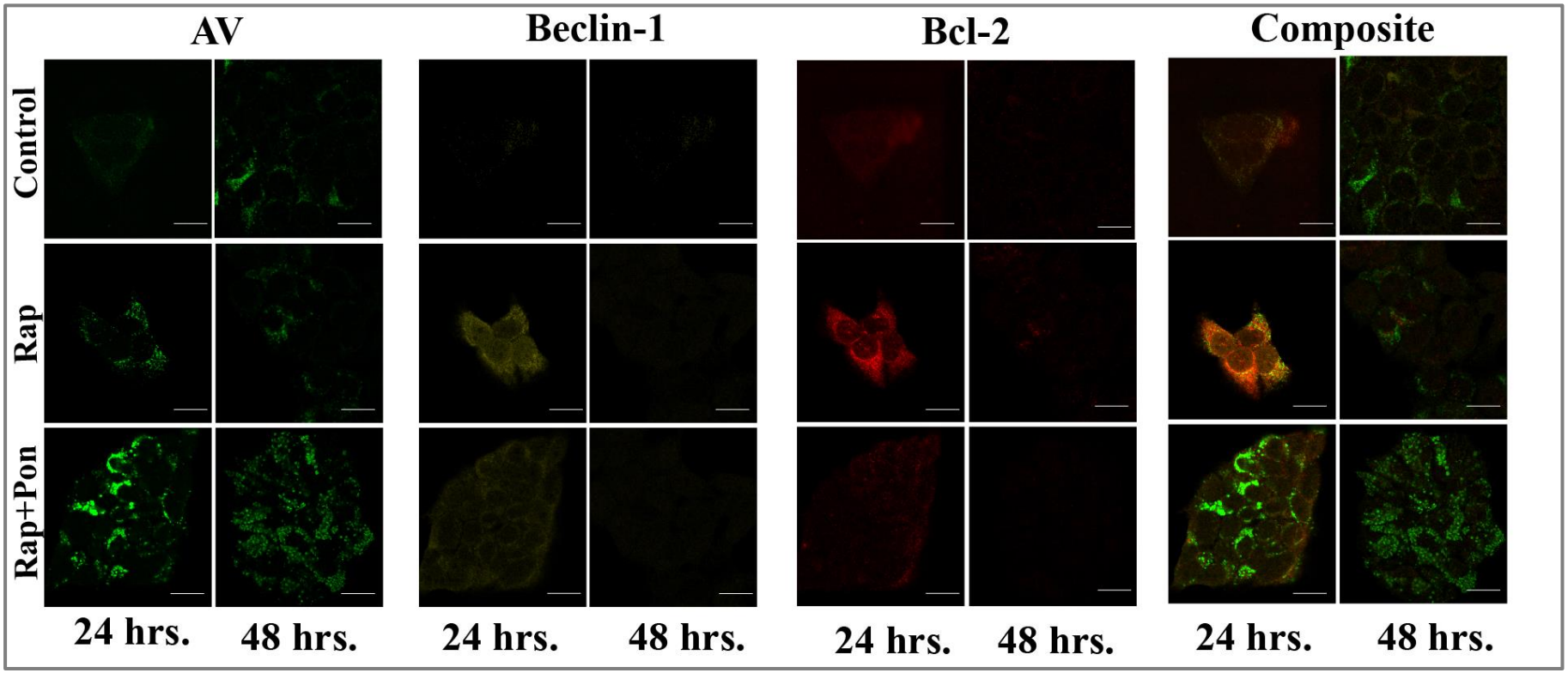

Figure 4.4. The provided panel showcases representative images of immunofluorescence of various proteins and vacuole with respect to treatment with Rapamycin in the presence and absence of PON. The figures provided represent immunofluorescence images displaying the staining of Beclin-1 and Bcl-2 in MCF-7 cells subjected to Rapamycin (Rap), a known positive regulator of autophagy, both with and without the addition of IC50 concentrations of PON, these treatments were carried out over 24 and 48-hour intervals. Notably, the autophagic vacuoles were identified and labeled through the utilization of CYTO-ID Autophagic vacuole detecting reagent, visualized in a distinct green colour. Furthermore, in-depth analysis of the provided images was conducted using ImageJ software. To quantitatively assess the fluorescence intensity, data were systematically calculated and subsequently presented in graphical form using GraphPad Prism software, with a dedicated figure for this purpose. These visual observations were captured at a significant magnification level of x600, and a scale bar accompanying the images denotes a measurement of 20 µm.

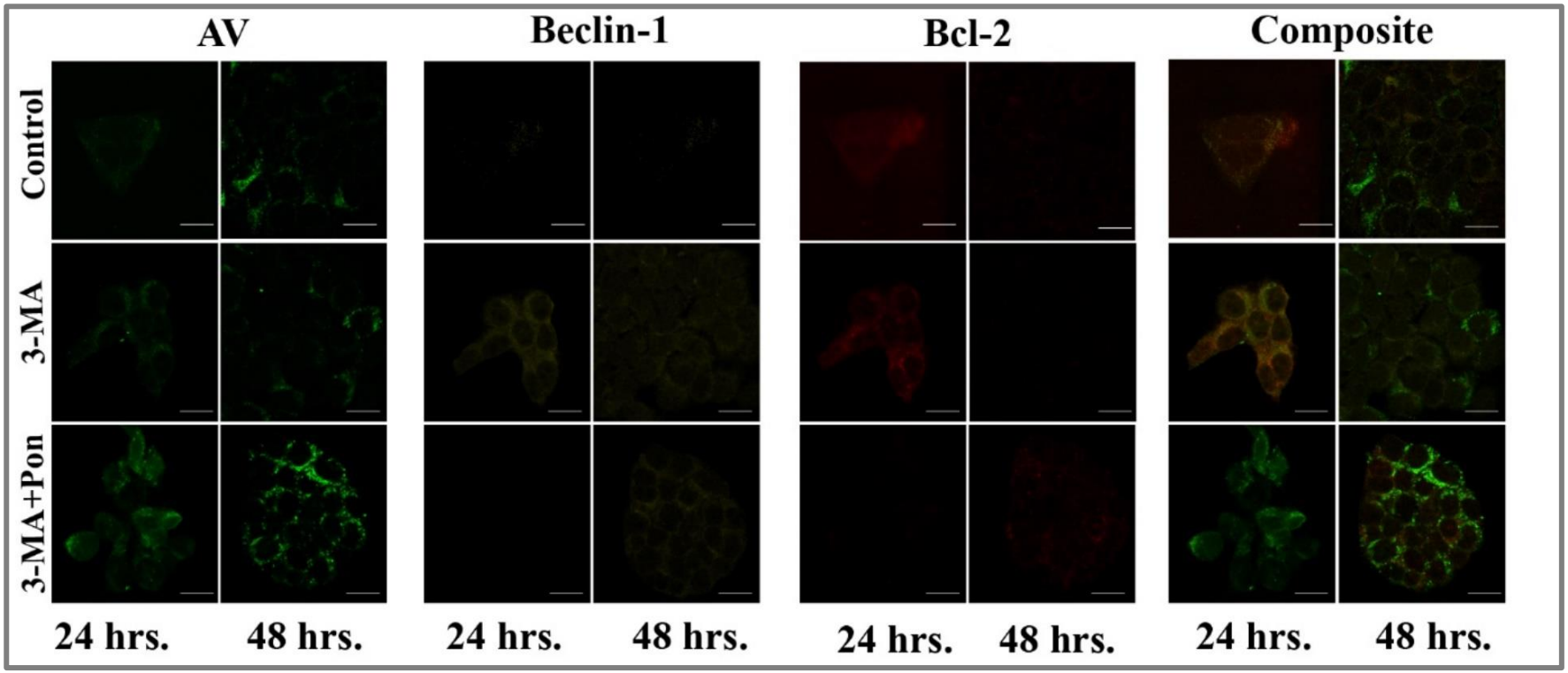

Figure 4.5. The panel displayed comprises representative immunofluorescence images of various proteins and vacuole with respect to treatment with 3-Methyladenine in the presence and absence of PON. Within these figures, immunofluorescence images illustrate the staining of Beclin-1 and Bcl-2 in MCF-7 cells exposed to 3-Methyladenine (3-MA), a well-known negative regulator of autophagy, both in the presence and absence of IC50 concentrations of Ponatinib (PON), these treatments spanned over 24 and 48-hour durations. Notably, autophagic vacuoles were identified and labeled using CYTO-ID Autophagic vacuole detecting reagent, which was rendered visible in a distinct green color. Furthermore, we conducted a comprehensive analysis of the provided images through the utilization of ImageJ software. To quantitatively evaluate the fluorescence intensity, data were meticulously calculated and subsequently represented graphically using GraphPad Prism software, with a dedicated figure exclusively dedicated to this purpose. It is essential to highlight that these visual observations were captured under substantial magnification, specifically at a level of x600, and a scale bar accompanying the images facilitated the measurement of 20 μm.

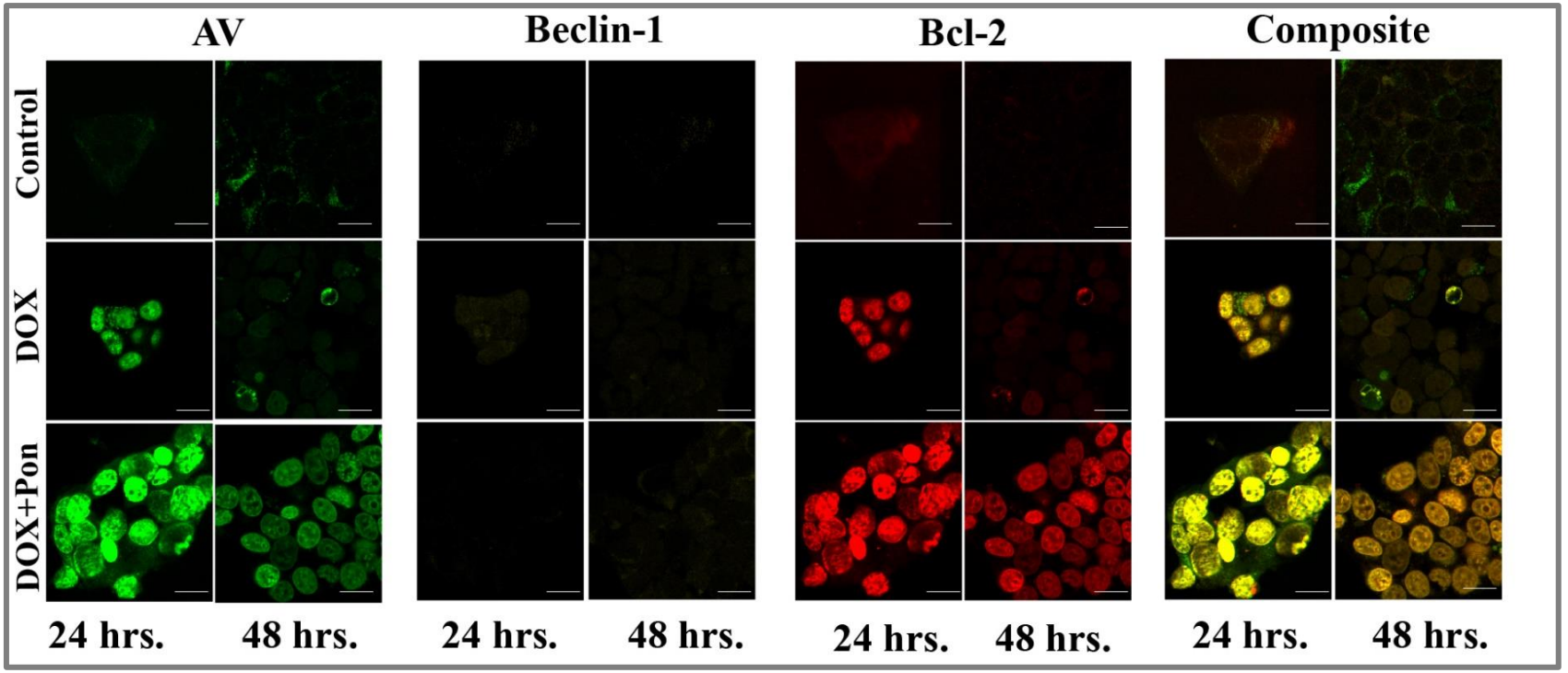

Figure 4.6. The presented panel encompasses a set of representative immunofluorescence images stained with several antibodies and dye. These figures showcase immunofluorescence images portraying the staining of Beclin-1 and Bcl-2 in MCF-7 cells following exposure to Doxorubicin (DOX), a well-established positive regulator of apoptosis, both in the presence and absence of IC50 concentrations of Ponatinib (PON), The experimental duration extended over 24 and 48-hour time frames. Notably, the visualization of autophagic vacuoles was achieved using CYTO-ID Autophagic vacuole detecting reagent, which manifested as a distinctive green fluorescence signal. Furthermore, a comprehensive analysis of the provided images was carried out through the utilization of ImageJ software. To quantitatively assess the fluorescence intensity, meticulous calculations were performed and the results were graphically represented using GraphPad Prism software. For this purpose, a dedicated figure was meticulously crafted. It is imperative to underscore that these visual observations were captured under a considerable level of magnification, specifically at a scale of x600. The accompanying scale bar in the images provided a precise measurement reference of 20 μm.

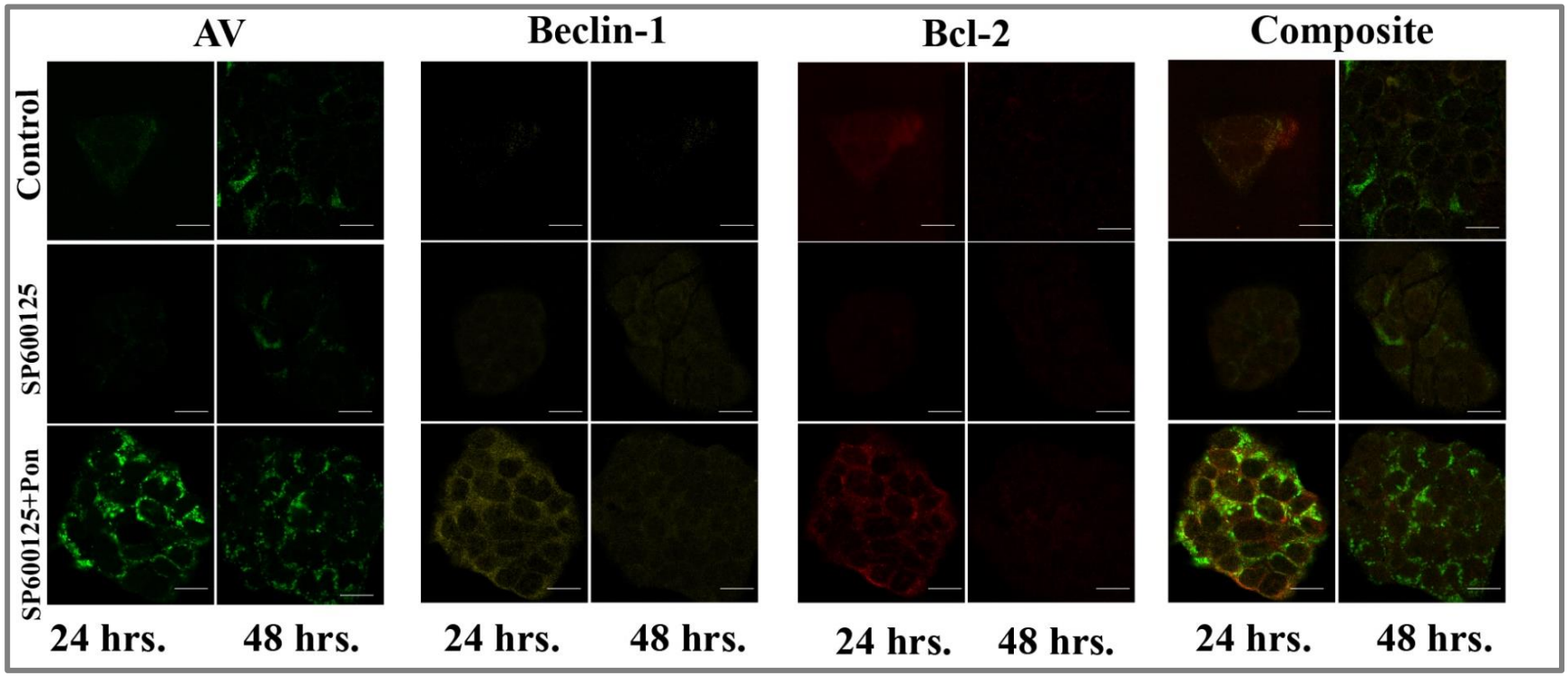

Figure 4.7. The presented panel comprises a series of representative immunofluorescence images. These figures display immunofluorescence images illustrating the staining of Beclin-1 and Bcl-2 in MCF-7 cells after exposure to SP600125, a well-established regulator capable of shifting the cell from autophagy to apoptosis, both in the presence and absence of Ponatinib (PON) at IC50 concentrations. The experiments were conducted. The experimental duration spanned 24 and 48-hour intervals. Notably, the visualization of autophagic vacuoles was facilitated using CYTO-ID Autophagic vacuole detecting reagent, producing a distinct green fluorescence signal. Subsequently, comprehensive image analysis was performed using ImageJ software. To quantitatively assess fluorescence intensity, meticulous calculations were executed, and the results were graphically presented via GraphPad Prism software. A dedicated figure was thoughtfully created for this purpose. It is important to emphasize that these visual observations were captured under a substantial level of magnification, specifically at a scale of x600, with the accompanying scale bar providing a precise measurement reference of 20 µm.

Our initial approach involved assessing the impact of Ponatinib, at both its IC50 and 2IC50 concentrations, on the levels of Beclin-1 (Figure 4.8). In Figure 4.8 B, as depicted in our western blot assay, the application of Ponatinib at its IC50 concentration exhibited an initial minor augmentation in the Beclin-1 protein levels at the 24-hour time point when compared with the control sample. However, as the assessment extended to the 48-hour mark, a discernible reduction in Beclin-1 protein levels became apparent. This trend persisted when utilizing Ponatinib at 2IC50 concentration, although noteworthy upregulation in Beclin-1 protein levels was observed at both the 24-hour and 48-hour time points. This observation suggests that Ponatinib treatment initially, at 24 hours, triggers an upregulation of autophagy, which subsequently diminishes with the progression of time (48 hours).

Concurrently, the influence of Ponatinib on Beclin-1 mRNA levels was examined as shown in Figure 4.8 A. Notably, when the IC50 concentration of Ponatinib was employed, Beclin-1 mRNA levels exhibited a downregulation at 48 hours relative to the 24-hour time point, although they remained comparatively lower than the control. In contrast, the application of Ponatinib at 2IC50 concentration led to a substantial increase in Beclin-1 mRNA levels at 48 hours compared to the levels observed at 24 hours. It is imperative to underscore that the regulation of the Beclin-1 and Bcl-2 interaction mediated by the chemotherapeutic agent Ponatinib predominantly manifested at the protein level. This decline in protein levels did not manifest a commensurate impact on the corresponding mRNA levels when Ponatinib was administered at its IC50 concentration. Conversely, the effect of Ponatinib on Beclin-1 mRNA levels was more pronounced at the 2IC50 concentration compared to the IC50 value, where the mRNA levels exhibited an increment at the 48-hour time point, conceivably as a compensatory response to the decline in Beclin-1 protein levels.

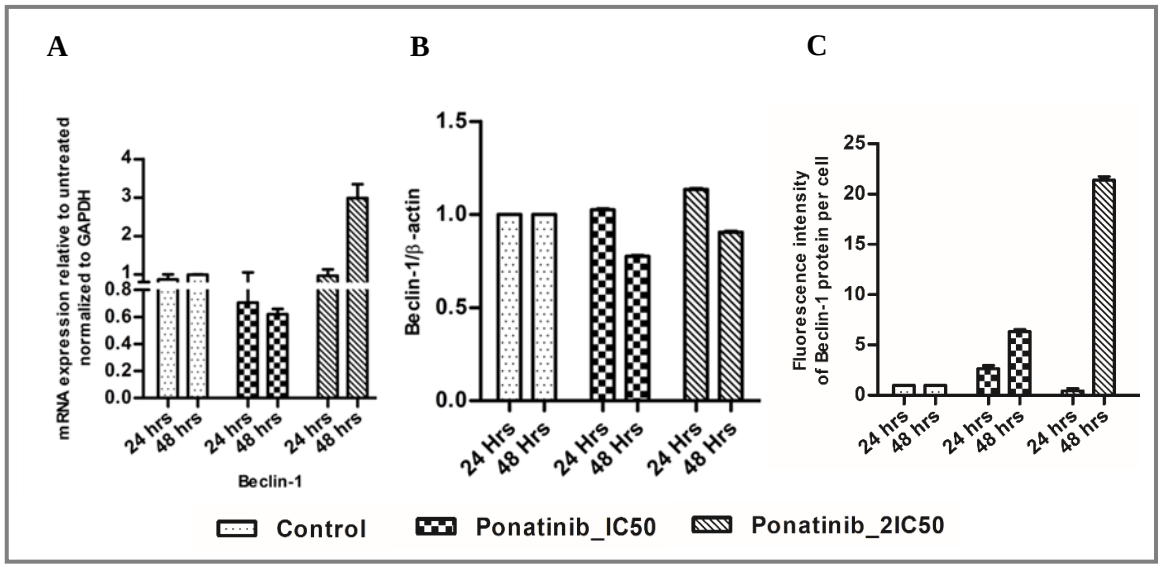

Figure 4.8. Effect of Ponatinib on Beclin-1 at mRNA and protein level. (A) The effect of PON, administered at both the IC50 and 2IC50 concentrations, on the alteration in Beclin-1 expression was evaluated. This analysis involved assessing the normalized fold change in Beclin-1 mRNA expression through real-time quantitative PCR. The data is double normalized to the control sample as well as the GAPDH gene, which was employed as loading control in the case of real-time q-PCR experiment. (**B)** The relative density value of the Beclin-1 protein level was determined using a western blot assay. The data is normalized to the control sample. β-Actin was employed as loading control in the case of western blot assay. (**C)** The effect of PON, administered at the IC50 and 2IC50 concentrations, on the alteration in Beclin-1 expression was evaluated by measuring the fluorescence intensity of Beclin-1 protein per cell and was quantified through an immunofluorescence assay employing confocal microscopy. The data is normalized to the control sample. The symbols and bars in the figure represent the mean values accompanied by the standard error of the mean (SEM) derived from three independent experimental replicates. Data analysis was carried out using GraphPad Prism and ImageJ software.

In our investigation, we conducted an assessment of the effect of Ponatinib on Beclin-1 protein levels using the immunofluorescence assay (Figure 4.8 C). Notably, when the IC50 concentration of Ponatinib was applied, there was an initial increase in the fluorescence intensity of Beclin-1 protein at the 24-hour time point. Subsequently, as the evaluation extended to the 48-hour mark, a further augmentation in the fluorescence intensity was observed. A parallel trend was observed when utilizing 2IC50 concentration of Ponatinib.

Our findings revealed a discrepancy between the levels of Beclin-1 protein assessed through Western blot assay and those obtained using the immunofluorescence assay. This incongruence in findings is consistent with existing literature, which reports varying outcomes in autophagy-mediated effects on selected proteins, often attributed to differences in the experimental methodologies employed (Dzietko *et al.* 2023). To provide a rationalization for this contradiction, it can be postulated that enzymatic digestion may augment the immunofluorescence intensity of proteins. The heightened immunofluorescence intensity observed in our results may not necessarily signify a genuine increase at the protein level. Instead, this enhanced immunofluorescence intensity can be attributed to an increase in degradation products resulting from the enzymatic breakdown of proteins. As a consequence of elevated degradation, there is an increased availability of reactive binding sites. Consequently, the localization of proteins using the immunofluorescence assay does not invariably align with the quantitative protein data derived from western blot analysis.

Also, the available literature underscores an intriguing aspect of Beclin-1 protein, where under conditions of heightened cellular stress surpassing a certain threshold, Beclin-1 protein undergoes Caspase-mediated cleavage (Wirawan *et al.* 2010). These cleaved products demonstrate a proclivity for translocating to critical cellular organelles, such as the mitochondria and nucleus, where they can trigger the process of apoptosis. Consequently, combining this valuable information from the literature with our experimental observations, it

is plausible to suggest that the enzymatic cleavage of Beclin-1 protein within the cell may lead to the exposure of multiple epitopes. This phenomenon, in turn, could contribute to the observed increase in antibody-based fluorescence at the 48-hour time point.

Beclin-1 is a crucial protein in the formation of autophagic vacuoles, which play a central role in the autophagy process. To comprehensively assess the level of autophagic vacuoles within the cells, the number of autophagic vacuoles (Avs) per cell was analysed (Figure 4.9). Treatment with Ponatinib (IC50) resulted in an initial increase in the number of autophagic vacuole at 24 hours. However, as time advanced (48 hours), there was a further increase in the number of AVs per cell. The same pattern was also observed at 2IC50 concentration of PON. This suggests that with the progression of time (48 hours), there is suppression in the autophagic flux, leading to the accumulation of already formed autophagic vacuoles within the cells. Consequently, this accumulation was reflected in increased number of autophagic vacuoles at 48 hours as compared to 24 hours.

Based on the Beclin-1 and number of autophagic vacuole levels, the data collectively indicates that upon the addition of Ponatinib, there is an initial boost in autophagy levels. However, over time, this is followed by the suppression of autophagic flux within the cell. These findings shed light on the complex dynamics of autophagy regulation and the potential therapeutic implications of targeting Beclin-1 with Ponatinib.

In our ongoing exploration, we are examining the effects of Ponatinib on two crucial proteins, Beclin-1 and Bcl-2. So far, we have focused on Beclin-1, but now we are looking at how Ponatinib affects Bcl-2 levels (Figure 4.10). A key element to comprehend here is that increased autophagy leads to the liberation of Bcl-2 from its binding with Beclin-1, resulting in the accumulation of free Bcl-2 in the cellular pool.

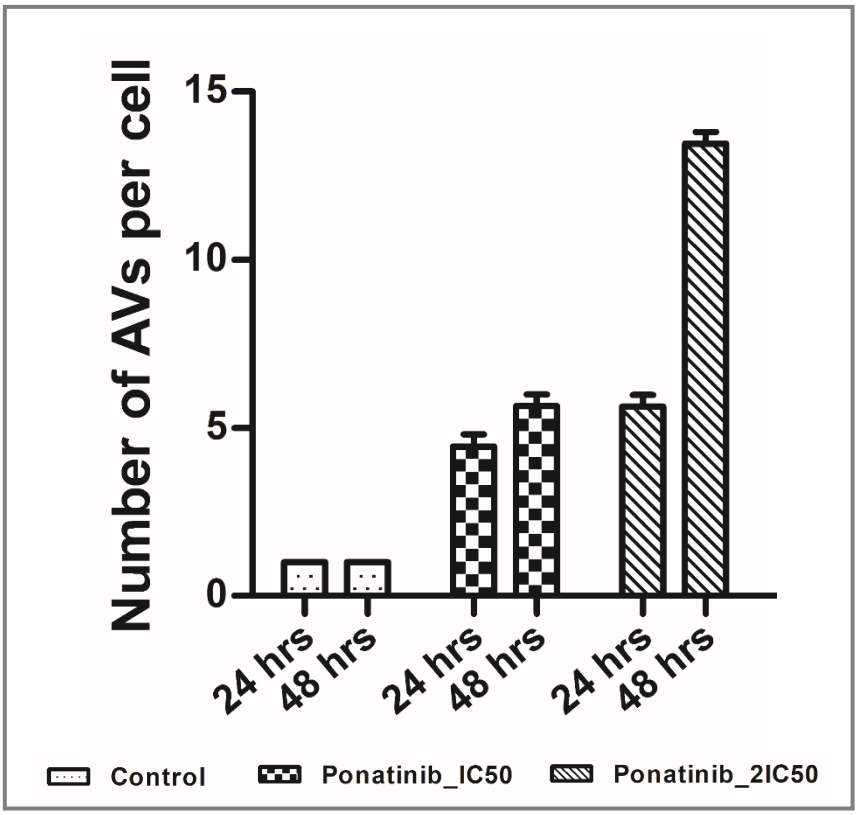

Figure 4.9. The Impact of Ponatinib on Autophagic vacuoles level in MCF-7 Cells. The effect of PON, administered at the IC50 and 2IC50 concentrations, on the alteration in number of autophagic vacuoles per cell was evaluated and quantified through an immunofluorescence assay conducted using confocal microscopy. The experimental design encompassed 24- and 48-hour intervals, with all data normalized to the control sample. The symbols and bars in the figure represent the mean values accompanied by the standard error of the mean (SEM) derived from three independent experimental replicates. Data analysis was carried out using GraphPad Prism and ImageJ software.

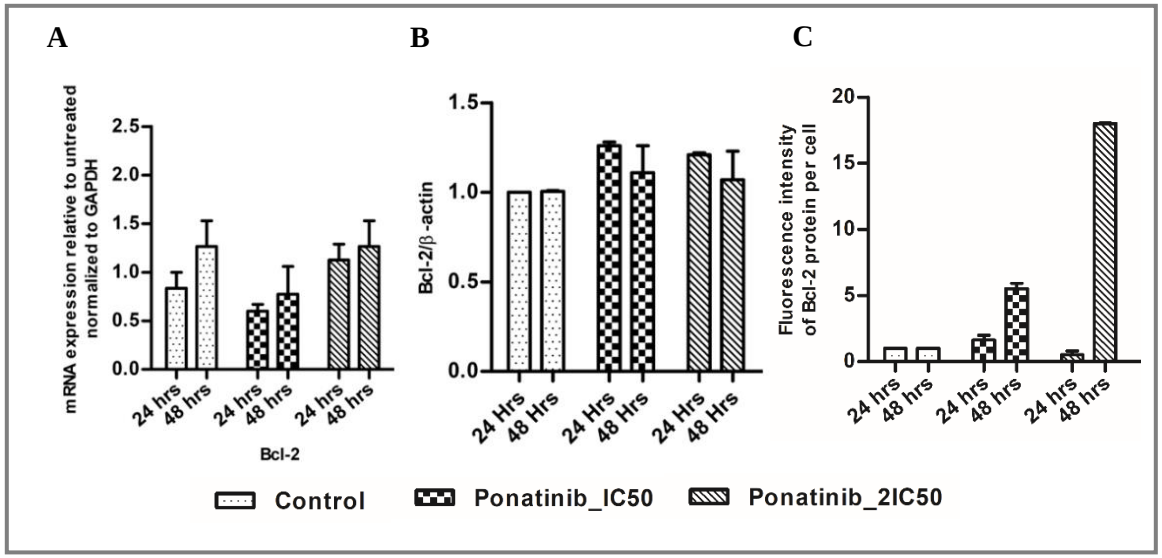

Figure 4.10. Effect of Ponatinib on Bcl-2 at mRNA and protein level. (**A)** The effect of PON, administered at both the IC50 and 2IC50 concentrations, on the alteration in Bcl-2 expression was evaluated. This analysis involved assessing the normalized fold change in Bcl-2 mRNA expression through real-time quantitative PCR. The data is double normalized to the control sample as well as the GAPDH gene, which was employed as loading control in the case of real-time q-PCR experiment. (**B)** The relative density value of the Bcl-2 protein level was determined using a western blot assay. The data is normalized to the control sample. β-Actin was employed as loading control in the case of western blot assay. (**C)** The effect of PON, administered at the IC50 concentration, on the alteration in Bcl-2 expression was evaluated by measuring the fluorescence intensity of Bcl-2 protein per cell and was quantified through an immunofluorescence assay employing confocal microscopy. The data is normalized to the control sample. The experimental design encompassed 24- and 48-hour intervals. The symbols and bars in the figure represent the mean values accompanied by the standard error of the mean (SEM) derived from three independent experimental replicates. Data analysis was carried out using GraphPad Prism and ImageJ software.

In a manner similar to our previous experiments, we employed both the IC50 and 2IC50 concentrations of Ponatinib to evaluate the levels of Bcl-2 in MCF7 cells. As illustrated in Figure 4.10 B, the graph represents the alterations in Bcl-2 protein levels as determined through western blot assay. Our observations revealed that the introduction of Ponatinib at the IC50 concentration led to an initial augmentation in the levels of free Bcl-2 protein within the cells at the 24-hour time point in comparison to the control sample. This phenomenon was subsequently followed by a conspicuous reduction in the quantity of free Bcl-2 protein at the 48-hour mark. A similar pattern in Bcl-2 protein levels was evident when the 2IC50 concentration of Ponatinib was administered to the cells. This distinctive pattern of an initial elevation followed by a subsequent decline in Bcl-2 protein levels suggests an initial upregulation in autophagy, with a subsequent suppression of autophagy as the experimental timeframe extended to 48 hours.

Moreover, at the Bcl-2 mRNA level (Figure 4.10 A), a marginal increase in the Bcl-2 mRNA was detected at 48 hours when the IC50 concentration of PON was used for treatment in the cells. It is noteworthy that the mRNA levels remained below the levels observed in the control sample. The similar pattern in the level of Bcl-2 mRNA was observed at 2IC50 concentration of PON. When considering these collective observations, a potential indication arises, aligning with our initial hypothesis: Autophagy is elevated at the 24-hour time point, followed by the inhibition of autophagic flux as time progresses to the 48-hour time point.

Further, the level of Bcl-2 protein was assessed through an immunofluorescence experiment in which cells exposed to both the concentrations, IC50 and 2IC50 of Ponatinib (Figure 4.10 C). The Bcl-2 protein was assessed once the treated cells were subjected to anti-Bcl-2 antibody staining. We could see the increased fluorescence intensity of Bcl-2 protein at 48 hours as compared to 24 hours when we checked both the IC50 and 2IC50 concentration of PON. Similar to the contradiction achieved at Beclin-1 protein level, we could also find

the similar contradiction in the western blot and immunofluorescence assay-based protein level. The literature reveals that as stress accumulates within the cell over time, a consequential upregulation of autophagy ensues. During this phase, an essential autophagy regulatory protein, AMBRA1, becomes involved in a binding interaction with Bcl-2, thereby facilitating the degradation of Bcl-2 (Yang *et al.* 2019). This observation provides a compelling rationale for the results we have obtained, particularly the increase in Bcl-2 fluorescence intensity at the 48-hour time point. It is plausible to infer that the degradation of Bcl-2 protein, as triggered by AMBRA1, may lead to the exposure of multiple epitopes on the Bcl-2 protein. This exposure of epitopes could in turn create multiple reactive binding sites for anti-Bcl-2 antibodies. Consequently, the observed elevation in fluorescence intensity of Bcl-2 at the 48-hour time point can be attributed to this enhanced availability of epitopes and binding sites, as facilitated by the autophagy regulatory processes initiated in response to prolonged cellular stress.

To further corroborate this pattern, we turned our attention to another significant player, the phospho-Bcl-2 protein, which exerts a pivotal influence on the regulation of autophagy and apoptosis (Figure 4.11). Notably, as increased autophagy prompts the release of Bcl-2 from Beclin-1 and subsequently leads to the phosphorylation of the liberated Bcl-2, primarily mediated by the JNK-1 signalling pathway. In the experiment, we found the phospho-Bcl-2 to be initially upregulated followed by a marginal decrease at 48 hours. The decrease in the phospho-Bcl-2 level was more pronounced when the cells were treated with 2IC50 concentration of PON. The observations suggest that the phospho-Bcl-2 level is aligning closely with our hypothesized trend.

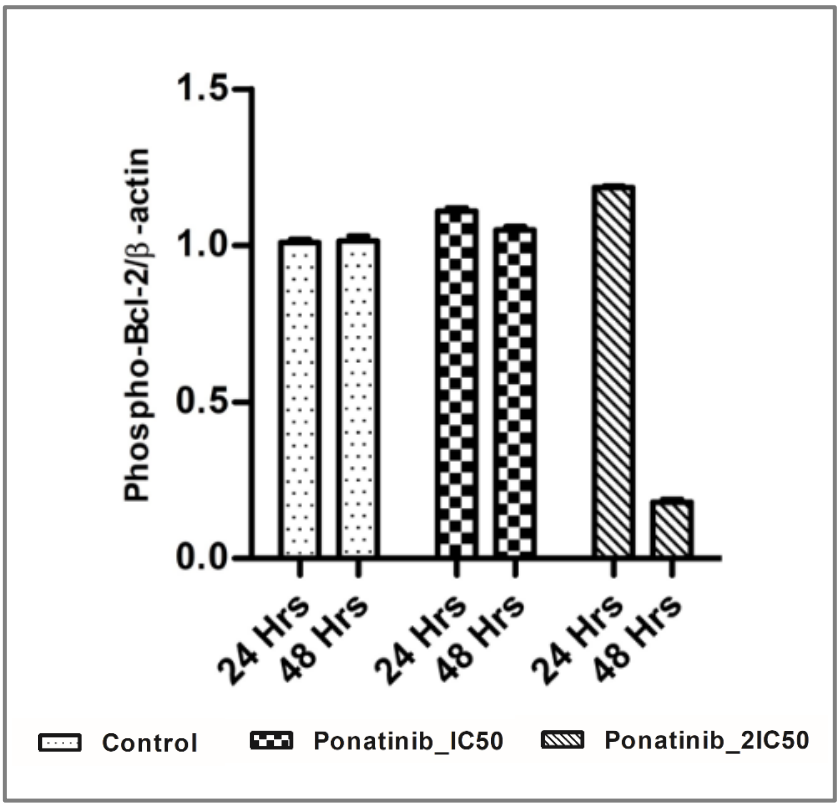

Figure 4.11. Effect of Ponatinib on Phospho-Bcl-2 at protein level. The role of phospho-Bcl-2 in these regulatory pathways was also addressed. The effect of PON, administered at both the IC50 and 2IC50 concentrations, on the alteration in Phospho-Bcl-2 expression was evaluated. The level of phospho-Bcl-2 was assessed by quantifying the relative density value through western blot analysis. The data is normalized to the control sample. β-Actin was employed as loading control in the case of western blot assay. The experimental design encompassed 24- and 48-hour intervals. The symbols and bars in the figure represent the mean values accompanied by the standard error of the mean (SEM) derived from three independent experimental replicates. Data analysis was carried out using GraphPad Prism and ImageJ software.

Having gleaned insights into the inhibition of autophagic flux at 48 hours, we sought to discern whether this inhibition triggered apoptosis. Our assessment of Cytochrome c mRNA levels using real time q-PCR experiment (Figure 4.12) yielded interesting observation indicating that, upon treating the cells with IC50 concentration of PON and as the timeline progresses to 48 hours, the levels of Cytochrome c mRNA substantially increased as compared to the level of cytochrome-c mRNA at 24 hours, however both the levels remained

less than the control sample. The similar trend yet more pronounced effect was observed in the 2IC50 concentration of PON. This observation strongly suggests that the inhibition of autophagic flux indeed triggers apoptosis within the cell.

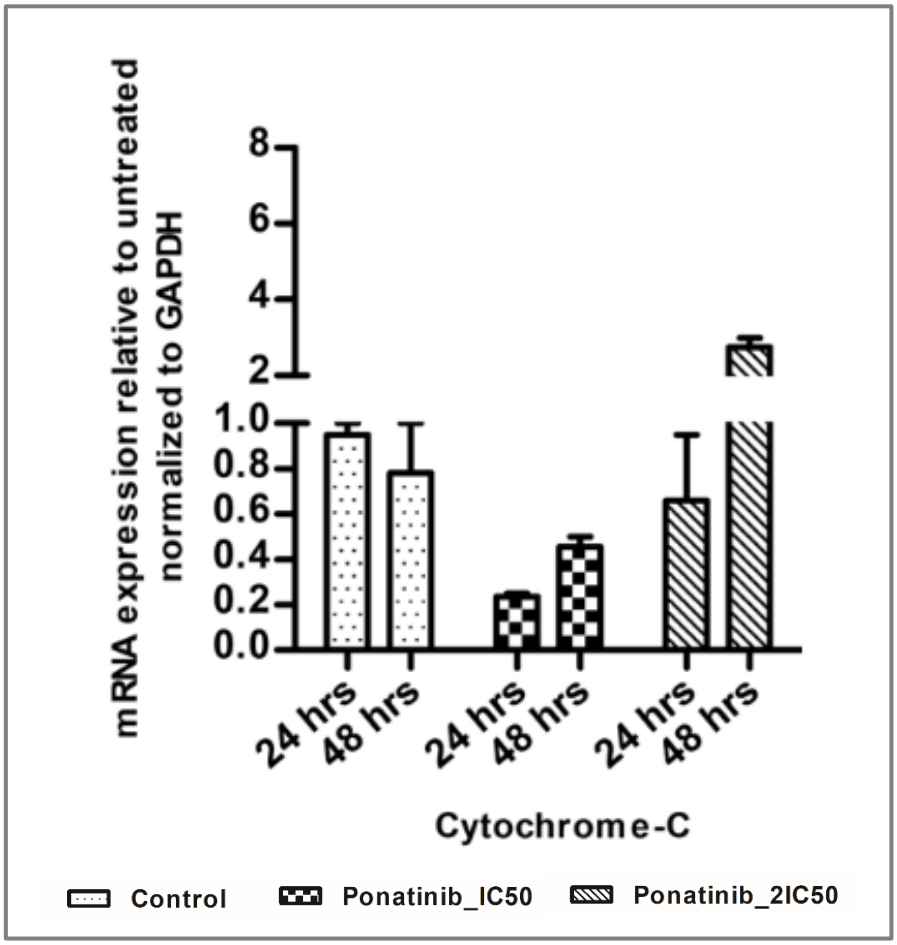

Figure 4.12. Effect of Ponatinib on Cytochrome-c at mRNA level. The role of Cytochrome-c in these regulatory pathways was also addressed. The effect of PON, administered at both the IC50 and 2IC50 concentrations, on the alteration in Cytochrome-c expression was evaluated. This analysis involved assessing the normalized fold change in Cytochrome-c mRNA expression through real-time quantitative PCR. The data is double normalized to the control sample as well as the GAPDH gene, which was employed as loading control in the case of real-time q-PCR experiment. The experimental design encompassed 24- and 48-hour intervals. The symbols and bars in the figure represent the mean values accompanied by the standard error of the mean (SEM) derived from three independent experimental replicates. Data analysis was carried out using GraphPad Prism and ImageJ software.

Collectively, our findings consistently affirm our hypothesis, suggesting that Ponatinib may initially provoke an increase in autophagy, followed by the onset of autophagic flux inhibition, ultimately culminating in apoptosis induction within the cellular milieu.

4.3.3 Rapamycin, a positive regulator of autophagy exerts synergistic effect on Ponatinib and triggers the inhibition in the autophagic flux and subsequently the apoptosis in MCF-7 cells.

To further corroborate our findings, we investigated the influence of Ponatinib on the interaction between Beclin-1 and Bcl-2 in the presence of pharmacological modulators of autophagy and apoptosis. Specifically, we employed Rapamycin, a known positive regulator of autophagy, in our study. In our investigation involving the co-administration of Ponatinib at its IC50 concentration and Rapamycin, while assessing key proteins using methods consistent with those employed in the previous section, several noteworthy observations were made (as depicted in Figure 4.13). Notably, in the context of Beclin-1 protein expression, as determined through Western blot analysis (Figure 4.13 B), an initial substantial upregulation of Beclin-1 protein levels was observed at the 24-hour time point following the combination treatment. However, this increase was followed by a decline in Beclin-1 protein levels at the 48-hour time point. Furthermore, in the immunofluorescence assay (Figure 4.13 C) for the combined treatment, the fluorescence intensity associated with Beclin-1 protein exhibited an augmentation at the 48-hour time point relative to the 24-hour time point. This particular trend indicates that, by the 48-hour time point, autophagic flux appears to be impeded. Additionally, the assessment of Beclin-1 mRNA levels (depicted in Figure 4.13 A) corroborated this trend, as it demonstrated an increase at the 48-hour time point compared to the 24-hour time point when considering the combined treatment. Upon examining the data at the 48-hour time point for Beclin-1 levels, considering both mRNA expression, protein levels assessed via the Western blot assay, and the results of the immunofluorescence assay, in the context of treatment with Rapamycin alone and the combined treatment of Rapamycin and

Ponatinib, a notable observation emerges. Specifically, it becomes evident that Rapamycin demonstrates a synergistic effect over Ponatinib in influencing Beclin-1 levels. This compelling finding motivates us to further analyse additional molecular markers to substantiate and validate this observation.

In our investigation, we extended our analysis to assess the impact of Rapamycin in combination with Ponatinib on the formation of autophagic vacuoles, as depicted in Figure 4.14. Notably, at the 24-hour time point, when considering both the treatment with Rapamycin alone and the combined treatment of Rapamycin and Ponatinib, an increase in the formation of autophagic vacuoles was observed. However, this increase was observed to be suppressed at the 48-hour time point in both treatment groups. It is important to acknowledge that this result does not align with our previous observations, indicating a discrepancy that warrants further investigation and analysis.

In light of the promising alignment of our Beclin-1 assessments with our initial hypothesis, we proceeded to investigate the combined effect of Rapamycin and Ponatinib on Bcl-2 levels, as illustrated in Figure 4.15. In the Western blot assay (Figure 4.15 B), when we considered the treatment group receiving Rapamycin and Ponatinib, a marginal reduction in Bcl-2 protein levels was observed at the 48-hour time point in comparison to the 24-hour time point. This observation implies that, by the 48-hour time point, there is a suppression of autophagic flux, mirroring the trend seen in the Beclin-1 protein levels. Furthermore, a congruent indication was noted within the same treatment group when assessing the immunofluorescence assay (Figure 4.15 C) at the 48-hour time point relative to the 24-hour time point. This suggests that the progression of time leads to the degradation of Bcl-2 protein, ultimately resulting in the inhibition of autophagic flux. Moreover, at the mRNA level, an increase in Bcl-2 mRNA levels was observed at the 48-hour time point when considering the Rapamycin and Ponatinib treatment group (Figure 4.15 A). This observation

reinforces the notion that Bcl-2 levels align with Beclin-1 levels, providing further support for our initial hypothesis.

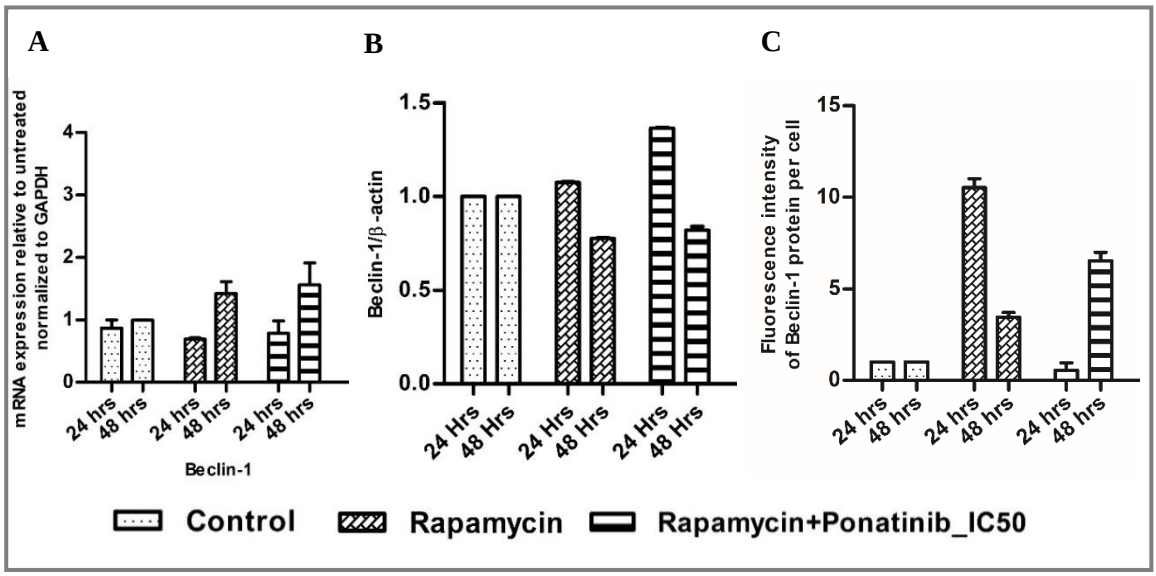

Figure 4.13. Impact of Rapamycin in the presence or absence of Ponatinib on Beclin-1 at both the mRNA and protein levels. (A) The influence of Rapamycin, either with or without PON, administered at the IC50 concentration, on Beclin-1 mRNA expression was analysed. This entailed measuring the normalized fold change in Beclin-1 mRNA levels through real-time quantitative PCR. The data was double normalized, considering both the control sample and the GAPDH gene as a loading control in the real-time q-PCR experiment. **(B)** The relative density value of Beclin-1 protein was determined using a western blot assay, with data normalized to the control sample. β-Actin served as the loading control in the western blot assay. **(C)** To evaluate the effect further on Beclin-1 expression, the fluorescence intensity of Beclin-1 protein per cell was quantified through an immunofluorescence assay utilizing confocal microscopy. For this experiment, the data was normalized to the control sample. The experimental design encompassed 24- and 48-hour intervals. The symbols and bars in the figure depict the mean values along with the standard error of the mean (SEM), derived from three independent experimental replicates. Data analysis was conducted using GraphPad Prism and ImageJ software.

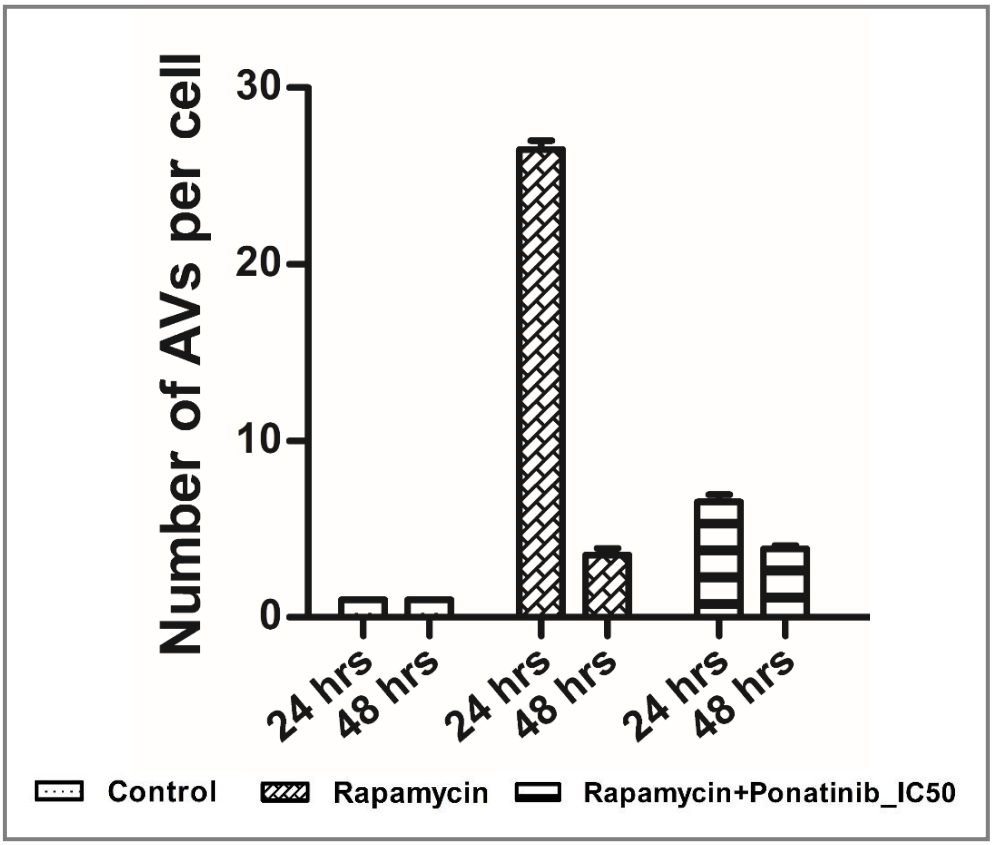

Figure 4.14. Effect of Rapamycin with/without Ponatinib on the number of autophagic vacuole level. This figure illustrates the number of autophagic vacuoles in MCF-7 cells treated with Rapamycin either alone or in combination with Ponatinib (PON) at its IC50 concentration. These measurements were conducted over 24 and 48-hour periods employing immunofluorescence assays with the aid of confocal microscopy. The number was quantified for autophagic vacuoles per cell using ImageJ software. Notably, the presented results are representative of three independent experiments, and the control group consisted of untreated cells. The symbols and bars in the figure depict the mean values along with the standard error of the mean (SEM), derived from three independent experimental replicates. Data analysis was conducted using GraphPad Prism and ImageJ software.

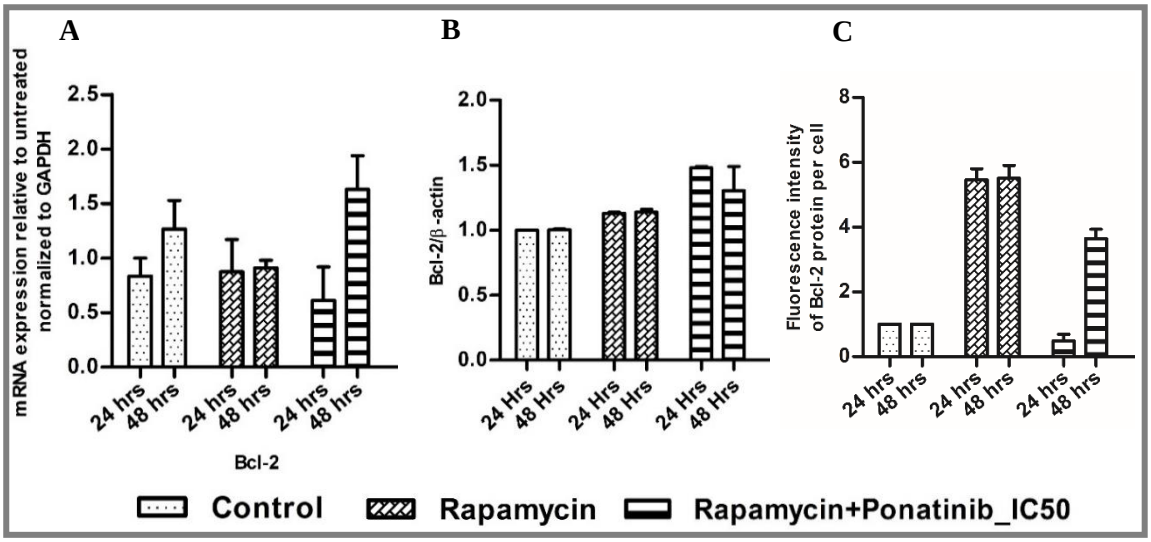

Figure 4.15. Impact of Rapamycin in the presence or absence of Ponatinib (PON) on Bcl-2 at both the mRNA and protein levels. (A) The influence of Rapamycin, either with or without PON, administered at the IC50 concentration, on Bcl-2 mRNA expression was analysed. This entailed measuring the normalized fold change in Bcl-2 mRNA levels through real-time quantitative PCR. The data was double normalized, considering both the control sample and the GAPDH gene as a loading control in the real-time q-PCR experiment. **(B)** The relative density value of Bcl-2 protein was determined using a western blot assay, with data normalized to the control sample. β-Actin served as the loading control in the western blot assay. **(C)** To evaluate the effect further, the fluorescence intensity of Bcl-2 protein per cell was quantified through an immunofluorescence assay utilizing confocal microscopy. For this experiment, the data was normalized to the control sample. All the experiments were conducted at 24 hrs and 48 hrs time points. The symbols and bars in the figure depict the mean values along with the standard error of the mean (SEM), derived from three independent experimental replicates. Data analysis was conducted using GraphPad Prism and ImageJ software.

To validate these observations, we also assessed the levels of phosphorylated Bcl-2 (phospho-Bcl-2) through western blot assay (Figure 4.16). Under the combined effect, it showed decreased level of phosph-Bcl-2 protein at 48 hours when it compared with 24-hour time point, which further corroborated our hypothesis. These results indicated that Rapamycin potentiated Ponatinib's attribute of inhibiting autophagic flux.

In order to determine whether the observed inhibition of autophagic flux led to apoptosis, we investigated the levels of cytochrome c mRNA, as depicted in Figure 4.17. Significantly, we noted a substantial increase in cytochrome c mRNA levels when Rapamycin was combined with Ponatinib at the 48-hour time point compared to the 24-hour time point. Importantly, this increase was notably more pronounced when compared to the treatment with Rapamycin alone. This finding suggests that the rapamycin very likely shows synergistic effect in conjunction with Ponatinib.

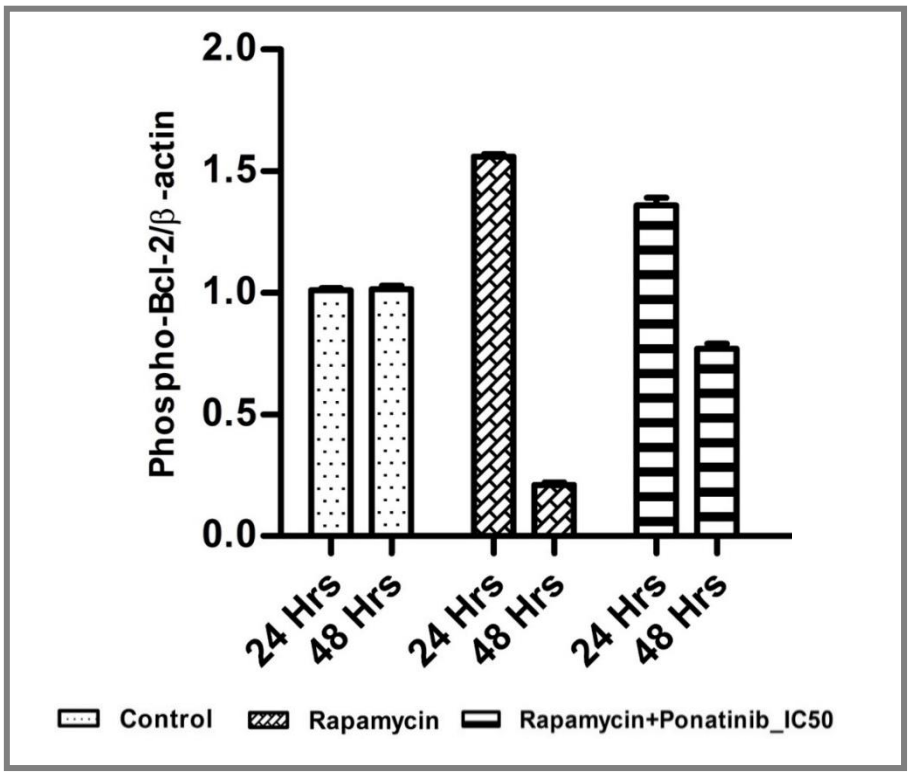

Figure 4.16. Influence of Rapamycin with or without Ponatinib on Phospho-Bcl-2 Protein Levels. This figure delves into the effect of Rapamycin, a well-established autophagy positive regulator with or without the presence of Ponatinib (PON) administered at the IC50 concentration, on the level of Phospho-Bcl-2, a key component in the regulatory pathways under investigation. The role of Phospho-Bcl-2 in these pathways is of particular interest and was thoroughly explored. The study involved the evaluation of changes in Phospho-Bcl-2 expression by quantifying the relative density value through western blot analysis. In this analysis, data was meticulously normalized to the control sample, and the loading control used for the western blot assay was β-Actin. The experimental design encompassed time intervals of both 24 and 48 hours. The symbols and bars within the figure represent the mean values along with the standard error of the mean (SEM) derived from three independent experimental replicates. Data analysis was conducted using GraphPad Prism and ImageJ software.

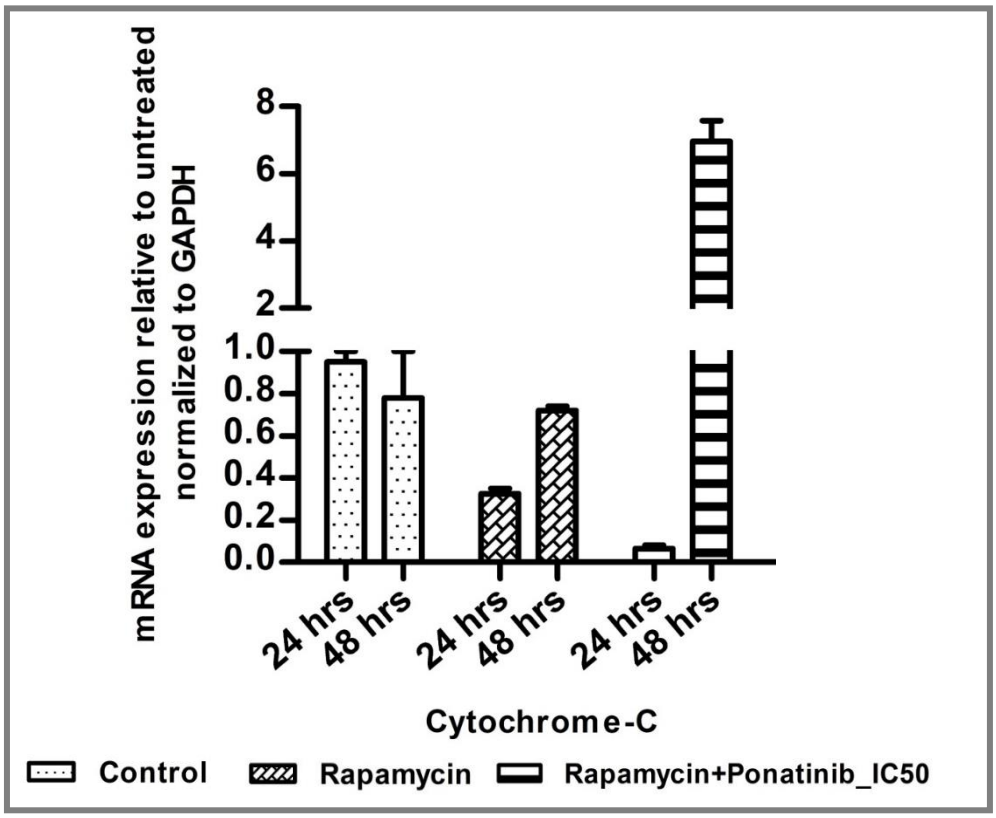

Figure 4.17. Impact of Rapamycin with or without Ponatinib on Cytochrome-c mRNA Levels. This figure offers insight into the effect of Rapamycin, a recognized autophagy regulator both in the presence and absence of Ponatinib (PON) at the IC50 concentration. The focus of the investigation is Cytochrome-c, a pivotal molecule in the apoptosis regulatory pathway. The study revolves around the assessment of alterations in Cytochrome-c expression by examining the normalized fold change in Cytochrome-c mRNA levels. In this process, the data is double normalized to the control sample and the GAPDH gene, serving as the loading control in the real-time q-PCR experiment. The experimental setup involves monitoring the effects at 24- and 48-hour intervals. The symbols and bars in the figure represent the mean values, along with the standard error of the mean (SEM), drawn from three independent experimental repetitions. Data analysis was executed through GraphPad Prism and ImageJ software.

In summary, our findings suggest that Rapamycin enhances Ponatinib's effect of triggering autophagic flux inhibition-mediated apoptosis in cancer cells, providing valuable insights into potential therapeutic strategies.

4.3.4 3-Methyladenine, a negative regulator of autophagy, helps identify the cell death is autophagy-mediated in MCF-7 cells.

To ascertain whether the cell death induced by Ponatinib over time is autophagy-mediated or involves an independent process of apoptosis, we conducted experiments involving the use of 3-Methyladenine (3-MA), a well-known autophagy inhibitor, in combination with IC50 concentration of Ponatinib. This allowed us to assess the combined effects of these drugs on time-dependent cell death, as illustrated in Figure 4.18.

As previously discussed in the introduction section, it is important to note that the *beclin-1* gene is frequently monoallelically deleted in most breast cancers, resulting in a downregulation of autophagy levels in cancer cells. When 3-MA was administered alone, our observations indicated that, at the 24-hour time point, Beclin-1 protein levels (Figure 4.18 B) were nearly equivalent to the control sample, consistent with Beclin-1 mRNA levels at 24 hours (Figure 4.18 A) and a slight increase in Beclin-1 protein fluorescence intensity at 24 hours in the immunofluorescence assay (Figure 4.18 C). Additionally, there was a negligible number of autophagic vacuoles at 24 hours (Figure 4.19). These results align with the Western blot analysis of Bcl-2 protein levels at 24 hours (Figure 4.20 B) when the 3-MA alone group was considered. Furthermore, at 24 hours, the cytochrome c mRNA level was found to be nearly equivalent to the control sample in the real-time q-PCR analysis (Figure 4.22). All these observations at 24 hours suggest that the effect of 3-MA is inhibiting autophagy, resulting in cancer cell survival.

However, as time progressed to 48 hours in the 3-MA alone group, there was a decrease in Beclin-1 protein levels (Figure 4.18 B), Bcl-2 protein levels (Figure 4.20 B), and phospho-Bcl-2 protein levels (Figure 4.21) as observed in the Western blot assay. Additionally, the number of autophagic vacuoles approached nearly the level of the control group at 48 hours (Figure 4.19). These findings indicate that prolonged exposure to 3-MA results in cell death,

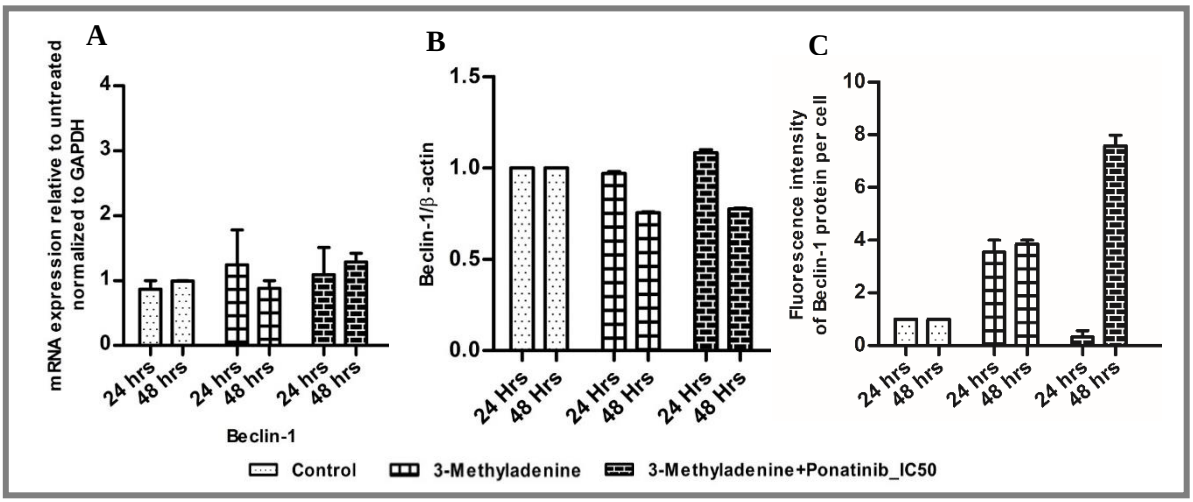

Figure 4.18. Impact of 3-Methyladenine, in the presence or absence of Ponatinib, on Beclin-1 at both the mRNA and protein levels. (A) The influence of 3-Methyladenine, either with or without PON, administered at the IC50 concentration, on Beclin-1 mRNA expression was analyzed. This entailed measuring the normalized fold change in Beclin-1 mRNA levels through real-time quantitative PCR. The data was double normalized, considering both the control sample and the GAPDH gene as a loading control in the real-time q-PCR experiment. **(B)** To evaluate the effect on Beclin-1 protein expression, the study involved quantifying the relative density value through western blot analysis. In this analysis, data was meticulously normalized to the control sample, and the loading control used for the western blot assay was β-Actin. **(C)** To evaluate the effect further, the fluorescence intensity of Bcl-2 protein per cell was quantified through an immunofluorescence assay utilizing confocal microscopy. For this experiment, the data was normalized to the control sample. The experimental design encompassed 24- and 48-hour intervals. The symbols and bars in the figure depict the mean values along with the standard error of the mean (SEM), derived from three independent experimental replicates. Data analysis was conducted using GraphPad Prism and ImageJ software.

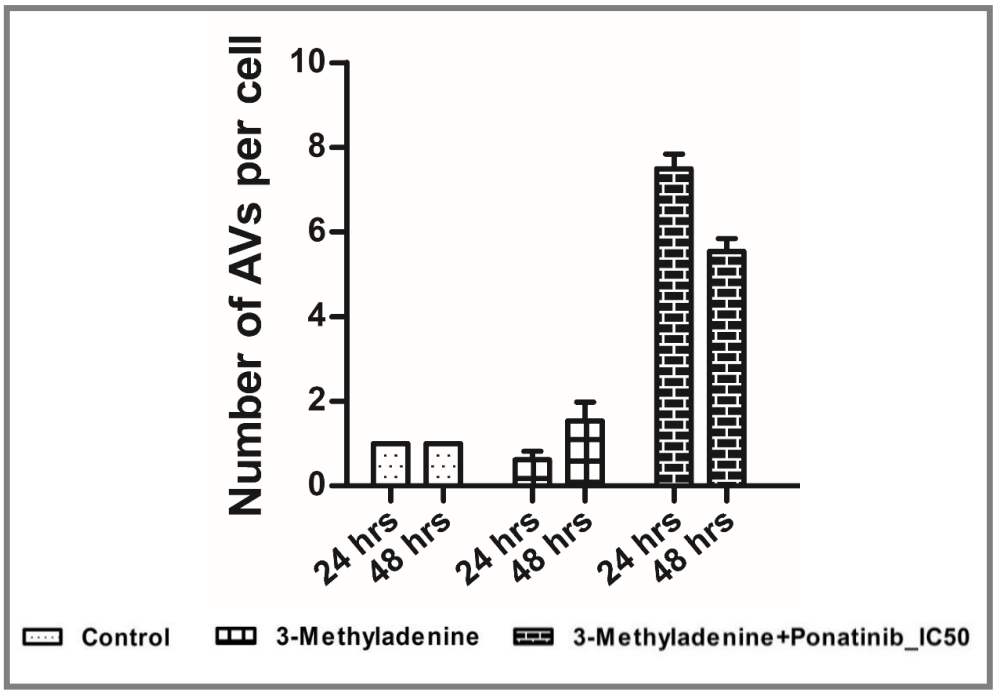

Figure 4.19. Effect of 3-Methyladenine with/without Ponatinib on the number of autophagic vacuole level. This figure illustrates the number of autophagic vacuoles in MCF-7 cells treated with 3-MA either alone or in combination with Ponatinib (PON) at its IC50 concentration. These measurements were conducted over 24 and 48-hour periods employing immunofluorescence assays with the aid of confocal microscopy. The number was quantified for autophagic vacuoles per cell using ImageJ software. Notably, the presented results are representative of three independent experiments, and the control group consisted of untreated cells. The symbols and bars in the figure depict the mean values along with the standard error of the mean (SEM), derived from three independent experimental replicates. Data analysis was conducted using GraphPad Prism and ImageJ software.

as reflected by the elevated cytochrome c mRNA levels depicted in Figure 4.22. Importantly, this cell death is not autophagy-mediated, as indicated by the number of autophagic vacuoles approaching control levels (Figure 4.19).

Furthermore, when 3-MA was combined with Ponatinib, we observed a marginal increase in Beclin-1 protein levels at 24 hours and subsequently a decrease in Beclin-1 protein levels at 48 hours (Figure 4.18 B). This trend in protein levels was consistent with Beclin-1 mRNA levels (Figure 4.18 A), which displayed a marginal increase in mRNA levels at 48 hours compared to 24 hours. The decrease in protein levels in the Western blot assay aligned with the increased degradation of Beclin-1 protein, resulting in an elevated fluorescence intensity of Beclin-1 protein at 48 hours in the immunofluorescence assay when considering the combination of 3-MA and Ponatinib (Figure 4.18 C).

Additionally, we assessed the number of autophagic vacuoles in the combined treatment group (Figure 4.19) and found that the number of autophagic vacuoles was significantly higher at 48 hours compared to the 3-MA alone group. Furthermore, the levels of Bcl-2 (at the protein and RNA levels) (Figure 4.20 A, B, and C) followed the same trend as Beclin-1 levels (at the protein and RNA levels). The phospho-Bcl-2 levels (Figure 4.21) were marginally decreased at 48 hours compared to 24 hours when considering the combined treatment.

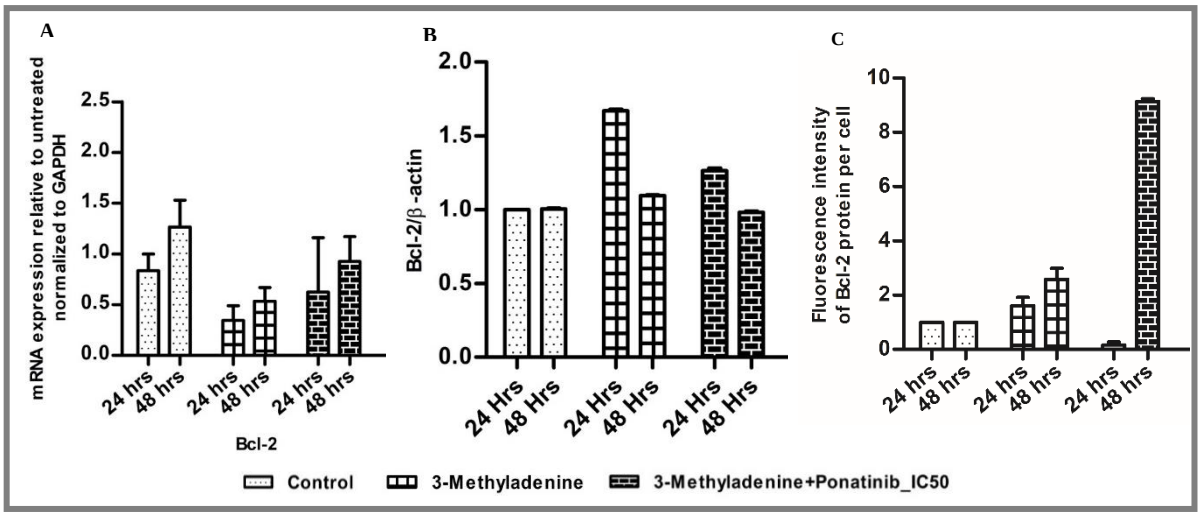

Figure 4.20. Impact of 3-Methyladenine in the Presence or Absence of Ponatinib on Bcl-2 at mRNA and Protein Levels. This figure explores the effects of 3-Methyladenine, a recognized negative regulator of autophagy, with or without the influence of Ponatinib (PON) when administered at the IC50 concentration, on Bcl-2. The analysis encompasses both mRNA and protein levels. **(A)** The influence of 3-Methyladenine in the Presence or Absence of PON is investigated by analyzing Bcl-2 mRNA expression. This involves the measurement of normalized fold changes in Bcl-2 mRNA levels through real-time quantitative PCR. The data is double-normalized, considering both the control sample and the GAPDH gene, which serves as a loading control in the real-time q-PCR experiment. **(B)** The assessment continues with the determination of the relative density value of Bcl-2 protein using a western blot assay, with the data normalized to the control sample. β-Actin is employed as the loading control in the western blot assay. **(C)** To evaluate the effect further, the fluorescence intensity of Bcl-2 protein per cell was quantified through an immunofluorescence assay utilizing confocal microscopy. For this experiment, the data was normalized to the control sample. The experimental design includes observations at 24- and 48-hour intervals. The symbols and bars in the figure represent the mean values alongside the standard error of the mean (SEM), derived from three independent experimental repetitions. Data analysis is carried out using GraphPad Prism and ImageJ software.

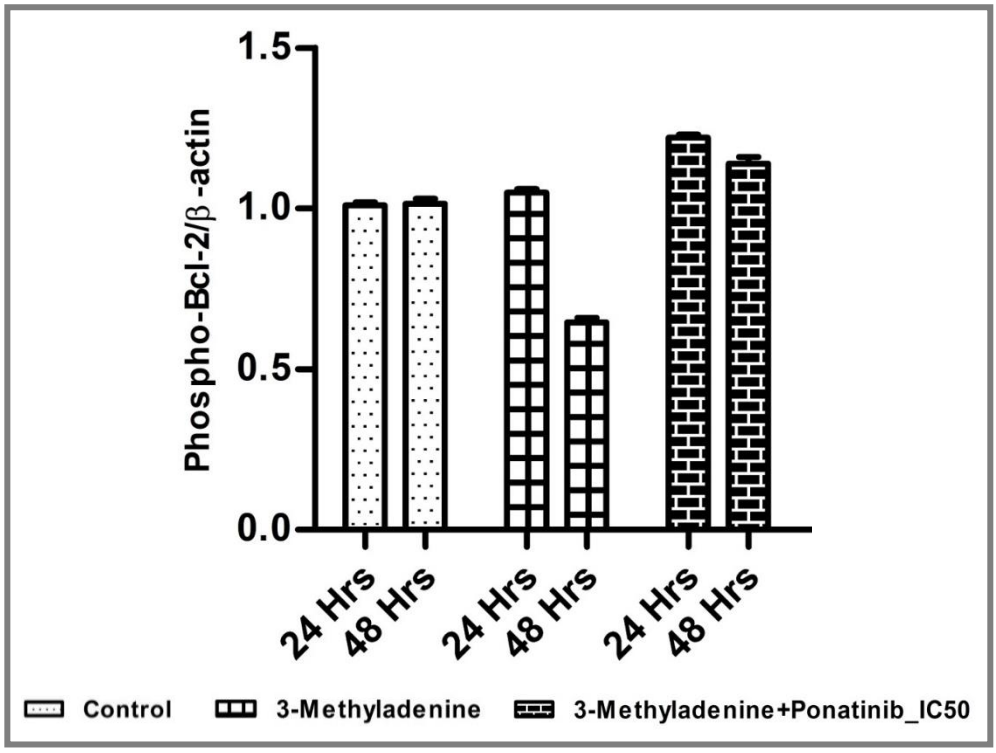

Figure 4.21. Impact of 3-Methyladenine with or without Ponatinib on Phospho-Bcl-2 Protein Levels. This figure is dedicated to understand the influence of 3-Methyladenine, a well-recognized negative regulator of autophagy, with or without the presence of Ponatinib (PON) when administered at the IC50 concentration, on the levels of Phospho-Bcl-2. Phospho-Bcl-2 is a vital component within the regulatory pathways under scrutiny. The investigation involves a comprehensive assessment of the alterations in Phospho-Bcl-2 expression. This analysis is accomplished by quantifying the relative density value via western blot analysis. The collected data is scrupulously normalized to the control sample. β-Actin is the chosen loading control for the western blot assay. The experimental design encompasses distinct time intervals, specifically at 24 and 48 hours, providing a comprehensive view of changes over time. The symbols and bars presented within the figure depict the mean values accompanied by the standard error of the mean (SEM), obtained from meticulous analysis involving three independent experimental replicates. Data analysis is executed with the aid of GraphPad Prism and ImageJ.

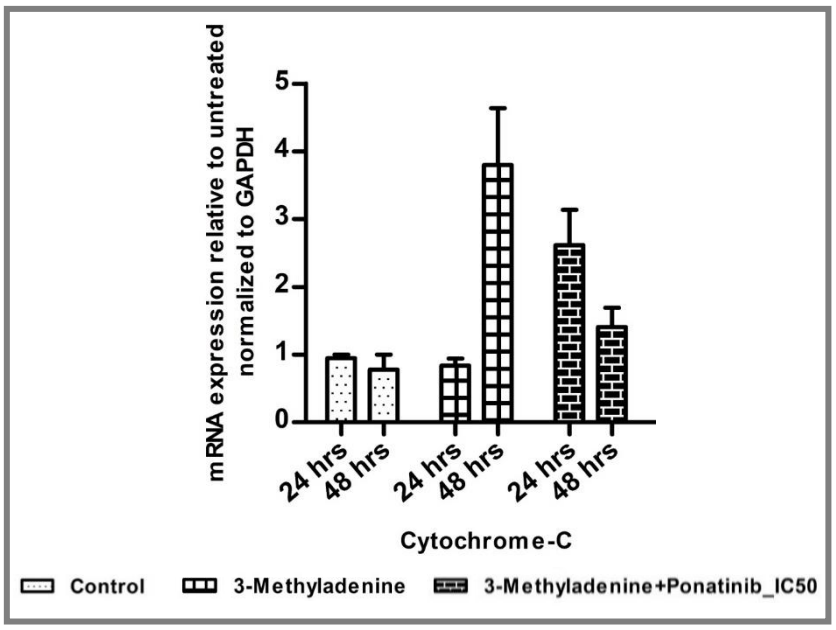

Figure 4.22. Influence of 3-Methyladenine with or without Ponatinib on Cytochrome-c at mRNA Level. In this figure, we explore the impact of 3-Methyladenine, a well-established inhibitor of autophagy, both in the presence and absence of on Ponatinib (PON) at its IC50 concentration, on Cytochrome-c expression at the mRNA level. Cytochrome-c plays a pivotal role in the regulatory pathways under examination. The analysis involves the evaluation of changes in Cytochrome-c mRNA expression, conducted via real-time quantitative PCR. The data is subjected to double normalization, referencing both the control sample and the GAPDH gene, which serves as a loading control in the real-time q-PCR experiment. The experimental framework encompasses time intervals of 24 and 48 hours, providing insights into changes occurring over these durations. The symbols and bars featured in the figure represent the mean values along with the standard error of the mean (SEM). These results are derived from a robust analysis based on three independent experimental replicates. Data analysis has been diligently executed through the utilization of sophisticated software tools, including GraphPad Prism and ImageJ.

Collectively, these results suggest that 3-MA is capable of inhibiting autophagy when administered alone. However, when 3-MA is combined with Ponatinib, Ponatinib appears to dominate, initially upregulating autophagy and subsequently accelerating the inhibition of autophagic flux over time. Notably, when we evaluated the combined effect of 3-MA and Ponatinib on cytochrome c mRNA levels (Figure 4.22), we observed a decrease in cytochrome c mRNA levels at 48 hours compared to 24 hours. This strongly indicates that the time-dependent cell death is actually mediated by autophagy. In conclusion, our findings suggest that upon the inhibition of autophagic flux by Ponatinib, the triggered cell death is indeed autophagy-mediated.

4.3.5 Doxorubicin, a positive regulator of apoptosis helps identifying that the cell death is not an independent apoptosis.

To further investigate whether Ponatinib-induced cell death is solely mediated by suppression in the autophagic flux or due to apoptosis, we introduced Doxorubicin, a known positive regulator of apoptosis, in combination with Ponatinib (IC50). We assessed Beclin-1 levels at both the mRNA and protein levels (Figure 4.23). in the western blot assay, we could see in the figure 4.23 B, our results demonstrated an increase in Beclin-1 protein expression at 24 hours and a subsequent decrease at 48 hours when dox was combined with PON. Moreover, in the immunofluorescence assay, the fluorescence intensity of Beclin-1 protein (Figure 4.23 C) was much higher when DOX was combined with PON. Furthermore, Beclin-1 mRNA levels (figure 4.23 A) showed an increase at 48 hours as compared to 24 hours. While Bcl-2 protein levels (Figure 4.24 B and C) exhibited a similar pattern just like Beclin-1 level (Figure 4.23 B and C), Bcl-2 mRNA levels (Figure 4.24 A) did not follow suit. Further, Phospho-Bcl-2 protein levels (figure 4.25) did not decrease at 48 hours. Additionally, cytochrome c mRNA levels (Figure 4.26) were much higher as compared to 24 hours when DOX was combined with PON.

The available scientific literature indicates that multiple anti-cancer pharmaceutical agents, such as Doxorubicin, exhibit the capacity to permeate the cellular nucleus, where they intercalate with DNA, resulting in subsequent DNA damage. In our experimental findings, a consistent pattern of nuclear localization was observed when the drug ponatinib was administered in conjunction with Doxorubicin. Consequently, a noteworthy increase in fluorescence intensity was noted within the nuclear region. These outcomes strongly imply that Doxorubicin exhibits a pronounced predominance in terms of nuclear penetration and nuclear localization compared to ponatinib. Also, the absence of autophagic vacuoles in the cell cytoplasm upon staining the cells with an autophagy vacuole staining dye is a critical

observation. This finding, when considered alongside our previous results, strongly suggests that Doxorubicin, when combined with Ponatinib, exerts a suppressive effect on autophagic flux as time progresses. However, the apoptosis triggered as a consequence of this suppression in autophagic flux (as reflected in the cytochrome c mRNA levels) is not primarily mediated by autophagy. Several key pieces of evidence support this conclusion: (i) Phospho-Bcl2 Protein Levels: The observation that there is no decrease in phospho-Bcl-2 protein levels, as assessed through Western blot analysis, indicates that the suppression of autophagic flux is not leading to apoptosis through the canonical Bcl-2-regulated pathway. (ii) Absence of Autophagic Vacuoles: The absence of autophagic vacuoles in the cell cytoplasm (as demonstrated in Figure 4.6) is a strong indication that the process of autophagy is indeed inhibited and not contributing to the observed cell death.

In light of these findings, it can be inferred that the cell death observed when Doxorubicin and Ponatinib are combined is primarily due to the dominance of Doxorubicin over Ponatinib. This is why, combination of Ponatinib and DOX did not induce higher levels of cell death compared to Doxorubicin alone (as evidenced by the cytochrome c mRNA levels at 48 hours when Doxorubicin was used as a single treatment). This suggests that Ponatinib-induced cell death is not solely attributable to apoptosis.

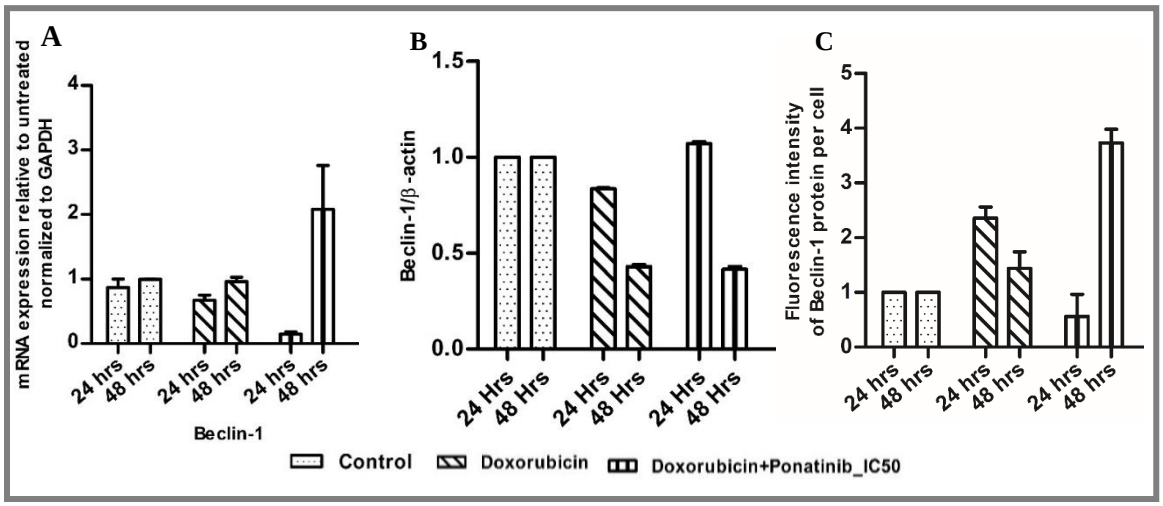

Figure 4.23. Impact of Doxorubicin, in the presence or absence of Ponatinib, on Beclin-1 at both the mRNA and protein levels. (A) The influence of Doxorubicin, either with or without PON, administered at the IC50 concentration, on Beclin-1 mRNA expression was analyzed. This entailed measuring the normalized fold change in Beclin-1 mRNA levels through real-time quantitative PCR. The data was double normalized, considering both the control sample and the GAPDH gene as a loading control in the real-time q-PCR experiment. **(B)** To evaluate the effect on Beclin-1 protein expression, the study involved quantifying the relative density value through western blot analysis. In this analysis, data was meticulously normalized to the control sample, and the loading control used for the western blot assay was β-Actin. **(C)** To evaluate the effect further, the fluorescence intensity of Beclin-1 protein per cell was quantified through an immunofluorescence assay utilizing confocal microscopy. For this experiment, the data was normalized to the control sample. The experimental design encompassed 24- and 48-hour intervals. The symbols and bars in the figure depict the mean values along with the standard error of the mean (SEM), derived from three independent experimental replicates. Data analysis was conducted using GraphPad Prism and ImageJ software.

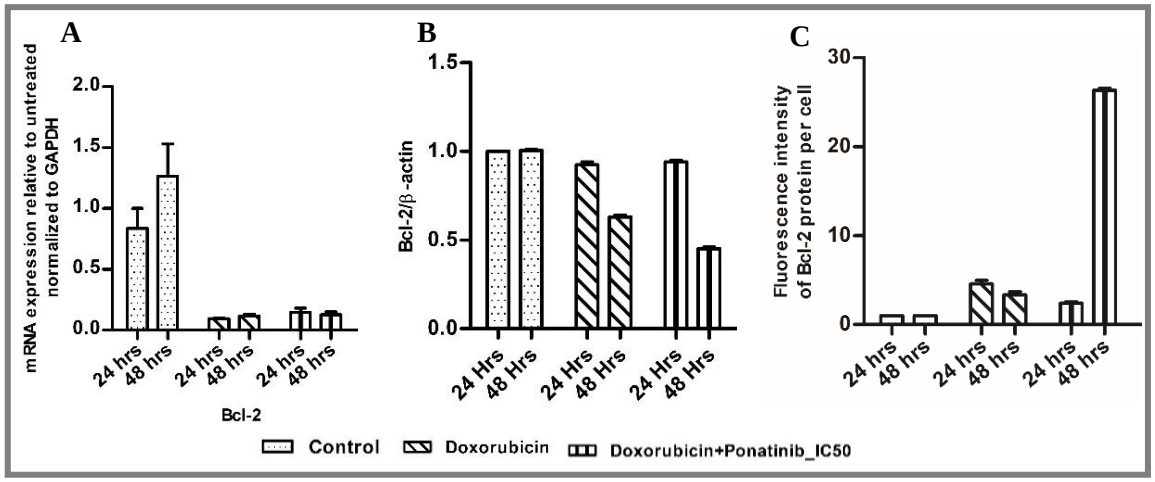

Figure 4.24. Impact of Doxorubicin in the Presence or Absence of Ponatinib on Bcl-2 at mRNA and Protein Levels. This figure explores the effects of Doxorubicin, a recognized positive regulator of apoptosis, with or without the influence of Ponatinib (PON) when administered at the IC50 concentration, on Bcl-2. The analysis encompasses both mRNA and protein levels. (**A)** The influence of 3-Methyladenine in the Presence or Absence of PON is investigated by analyzing Bcl-2 mRNA expression. This involves the measurement of normalized fold changes in Bcl-2 mRNA levels through real-time quantitative PCR. The data is double-normalized, considering both the control sample and the GAPDH gene, which serves as a loading control in the real-time q-PCR experiment. **(B)** The assessment continues with the determination of the relative density value of Bcl-2 protein using a western blot assay, with the data normalized to the control sample. β-Actin is employed as the loading control in the western blot assay. **(C)** To evaluate the effect further, the fluorescence intensity of Bcl-2 protein per cell was quantified through an immunofluorescence assay utilizing confocal microscopy. For this experiment, the data was normalized to the control sample. The experimental design includes observations at 24- and 48-hour intervals. The symbols and bars in the figure represent the mean values alongside the standard error of the mean (SEM), derived from three independent experimental repetitions. Data analysis is carried out using GraphPad Prism and ImageJ software.

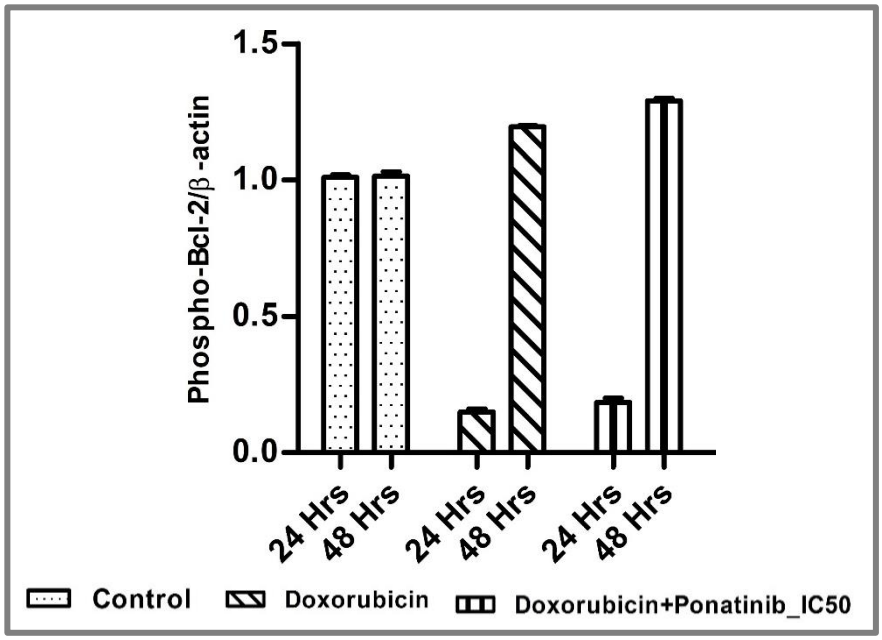

Figure 4.25. Impact of Doxorubicin with or without Ponatinib on Phospho-Bcl-2 Protein Levels. This figure is dedicated to understand the influence of Doxorubicin, a well-recognized positive regulator of apoptosis, with or without the presence of Ponatinib (PON) when administered at the IC50 concentration, on the levels of Phospho-Bcl-2. Phospho-Bcl-2 is a vital component within the regulatory pathways under scrutiny. The investigation involves a comprehensive assessment of the alterations in Phospho-Bcl-2 expression. This analysis is accomplished by quantifying the relative density value via western blot analysis. The collected data is scrupulously normalized to the control sample. β-Actin is the chosen loading control for the western blot assay. The experimental design encompasses distinct time intervals, specifically at 24 and 48 hours, providing a comprehensive view of changes over time. The symbols and bars presented within the figure depict the mean values accompanied by the standard error of the mean (SEM), obtained from meticulous analysis involving three independent experimental replicates. Data analysis is executed with the aid of GraphPad Prism and ImageJ.

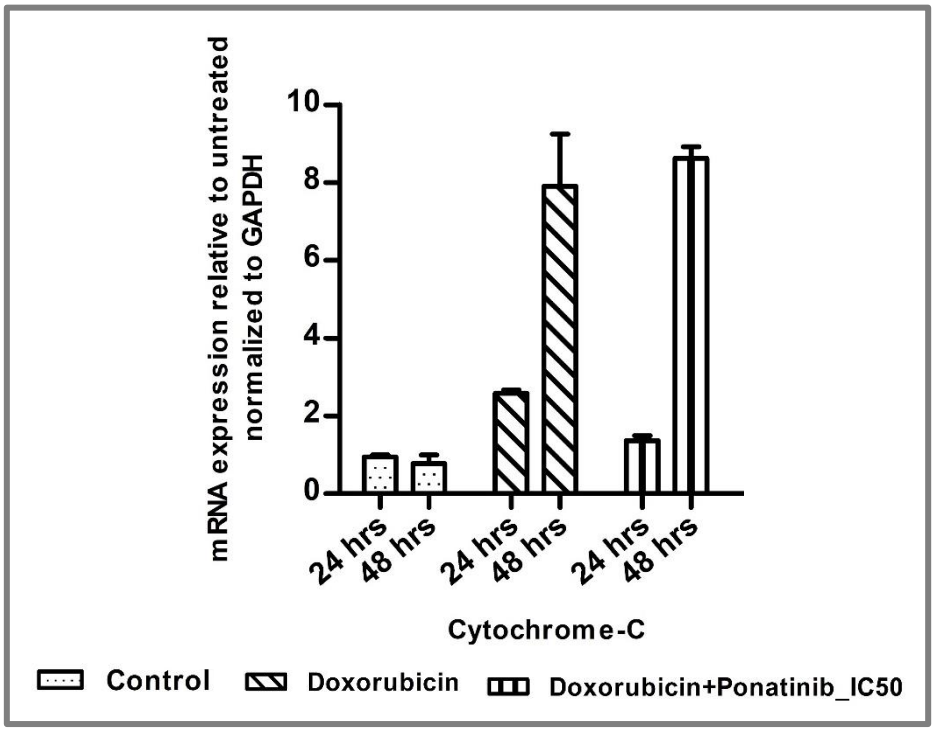

Figure 4.26. Influence of Doxorubicin with or without Ponatinib on Cytochrome-c at mRNA Level. In this figure, we explore the impact of Doxorubicin, a well-established positive regulator of apoptosis, both in the presence and absence of on Ponatinib (PON) at its IC50 concentration, on Cytochrome-c expression at the mRNA level. Cytochrome-c plays a pivotal role in the regulatory pathways under examination. The analysis involves the evaluation of changes in Cytochrome-c mRNA expression, conducted via real-time quantitative PCR. The data is subjected to double normalization, referencing both the control sample and the GAPDH gene, which serves as a loading control in the real-time q-PCR experiment. The experimental framework encompasses time intervals of 24 and 48 hours, providing insights into changes occurring over these durations. The symbols and bars featured in the figure represent the mean values along with the standard error of the mean (SEM). These results are derived from a robust analysis based on three independent experimental replicates. Data analysis has been diligently executed through the utilization of sophisticated software tools, including GraphPad Prism and ImageJ.

4.3.6 SP600125, a regulator which drive the cell's fate from autophagy to apoptosis, does not show synergistic effect on Ponatinib.

To confirm that autophagy-mediated cell death in cancer cells is indeed autophagy-mediated rather than an independent apoptosis, we employed SP600125, an inhibitor of stress-driven JNKs known to promote autophagy-mediated apoptosis. In the combined treatment of SP600125 and Ponatinib (IC50), we assessed several molecular markers, including Beclin-1 levels at both the mRNA and protein levels, autophagic vacuoles, Bcl-2 levels, phospho-Bcl-2 protein levels, and cytochrome c mRNA levels.

In the SP600125 alone treatment group, we observed that Beclin-1 protein levels initially increased at 24 hours, followed by a decrease at 48 hours (Figure 4.27 B). This decrease in Beclin-1 protein levels was consistent with elevated fluorescence intensity of Beclin-1 protein at 48 hours in the immunofluorescence assay (Figure 4.27 C). Beclin-1 mRNA levels were also found to be higher at 48 hours compared to 24 hours (Figure 4.24 A). In the same treatment group, the analysis of autophagic vacuoles showed a slight increase at 48 hours (Figure 4.28). The trends in Bcl-2 levels, both at the RNA and protein levels, paralleled the Beclin-1 levels (Figure 4.29 A, B, and C). Phospho-Bcl-2 protein levels showed a decreased level at 48 hours compared to 24 hours in the same treatment group, and cytochrome c mRNA levels displayed a massive increase at 48 hours (Figure 4.30 and Figure 4.31). These observations strongly suggest that SP600125 alone treatment has the potential to increase autophagy-mediated cell death.

We also assessed the effect of SP600125 in combination with Ponatinib (IC50). In this combined treatment group, we evaluated the same markers, including Beclin1 mRNA and protein levels, autophagic vacuoles, Bcl-2 levels, phospho-Bcl-2 protein levels, and cytochrome c mRNA levels. For Beclin-1 levels, we observed an increase in Beclin-1 mRNA levels at 48 hours compared to 24 hours (Figure 4.27 A), and at the protein level, there was

an increase in the fluorescence intensity of Beclin-1 protein at 48 hours compared to 24 hours. However, in contrast to the SP600125 alone treatment, we did not observe a decrease in Beclin-1 protein levels at 48 hours in the Western blot assay (Figure 4.27 B). The number of autophagic vacuoles showed a decreased number at 48 hours compared to 24 hours (Figure 4.28). Bcl-2 levels (both at the RNA and protein levels) and phospho-Bcl-2 protein levels displayed similar trends to Beclin-1 levels (Figure 4.29 A, B, C, and Figure 4.30). Cytochrome c mRNA levels notably increased at 48 hours compared to 24 hours (Figure 4.31). These findings suggest that Ponatinib also has the potential to induce autophagy-mediated cell death, with subsequent progression to apoptosis in cancer cells. However, it's important to note that the addition of SP600125 did not synergistically enhance this effect when combined with Ponatinib.

In summary, through a comprehensive assessment of Ponatinib in combination with various pharmacological modulators of autophagy and apoptosis, our findings suggest that Ponatinib has the potential to induce autophagy-mediated cell death, with subsequent progression to apoptosis in cancer cells.

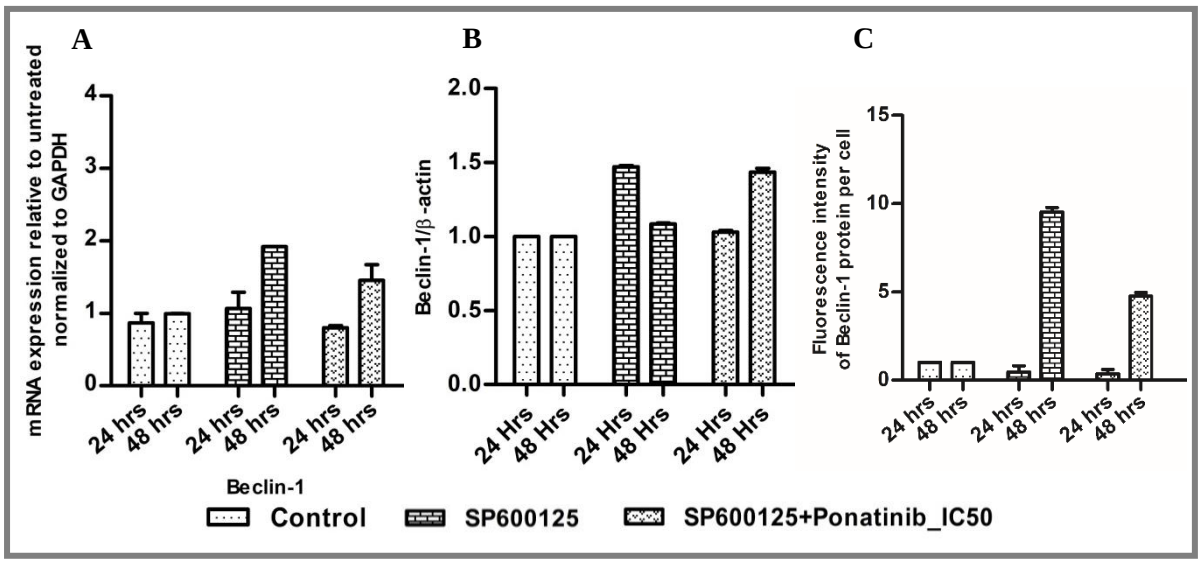

Figure 4.27. Impact of SP600125 on Beclin-1 at mRNA and Protein Levels with or without Ponatinib. This figure delves into the influence of SP600125, a recognized cellular fate regulator capable of shifting the balance between autophagy and apoptosis. The effects of SP600125 are examined both in the presence and absence of Ponatinib (PON) at its IC50 concentration. **(A)** The influence of SP600125, with or without PON, on Beclin-1 mRNA expression was thoroughly investigated. This analysis encompassed the quantification of normalized fold changes in Beclin-1 mRNA levels through real-time quantitative PCR. To ensure data accuracy, double normalization was conducted by referencing both the control sample and the GAPDH gene, which functioned as a loading control in the real-time q-PCR experiment. **(B)** Beclin-1 protein levels were scrutinized by assessing relative density values through western blot analysis. Data normalization was carried out in relation to the control sample, with β-Actin serving as the loading control in the western blot assay. **(C)** To probe the effect of SP600125, with or without PON at the IC50 concentration, on Beclin-1 expression, the fluorescence intensity of Beclin-1 protein per cell was quantified via an immunofluorescence assay employing confocal microscopy. The data was subsequently normalized to the control sample. The experimental design spanned 24- and 48-hour intervals, providing insights into the temporal dynamics of Beclin-1 expression. The symbols and bars featured in the figure represent the mean values accompanied by the standard error of the mean (SEM). These values were calculated based on data obtained from three independent experimental replicates. The analysis of the data was meticulously conducted using GraphPad Prism and ImageJ software tools.

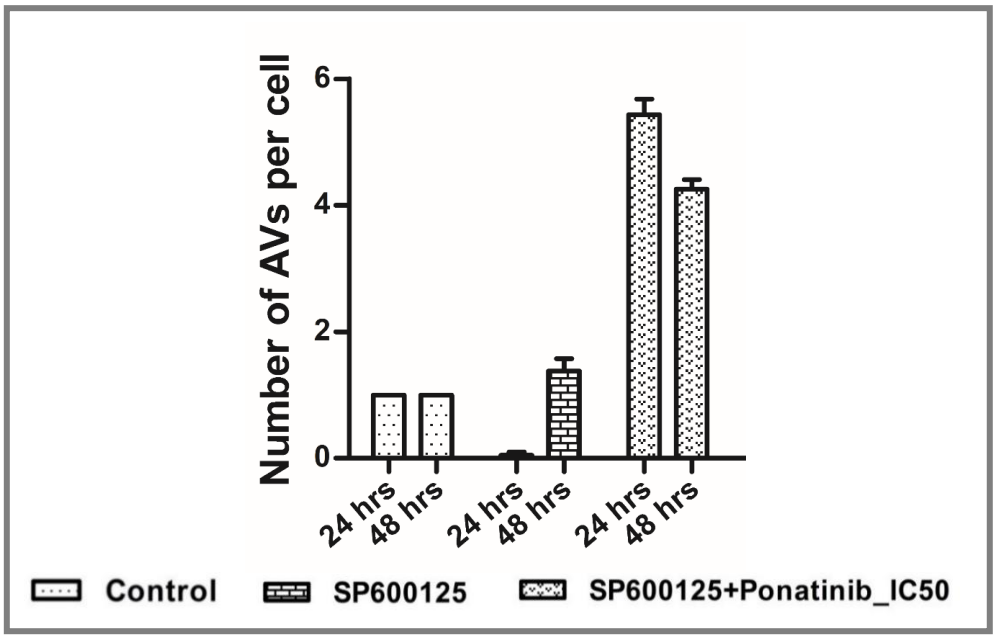

Figure 4.28. Impact of SP600125 with/without Ponatinib on the level of number of autophagic vacuole. This figure provides insights into the effect of SP600125 in the presence or absence of Ponatinib (PON) at its IC50 concentration on the level of autophagic vacuole. The assessment involves measuring the number of autophagic vacuoles within MCF-7 cells. These experiments extended over 24- and 48-hour durations and were conducted using immunofluorescence assays aided by confocal microscopy. The figure illustrates the number of autophagic vacuoles in MCF-7 cells following treatment with SP600125 either as a sole agent or in combination with Ponatinib (PON) at its IC50 concentration. The quantification of number was performed for autophagic vacuoles per cell, and this analysis was carried out using ImageJ software. The study involved a 24-hour and 48-hour experimental design, allowing for the examination of how autophagic vacuole levels change over time in response to the treatments. The control group for comparison consisted of untreated cells. The symbols and bars in the figure represent the mean values along with the standard error of the mean (SEM), which were calculated based on data obtained from three independent experimental replicates. The analysis of the data was meticulously conducted using GraphPad Prism and ImageJ software tools.

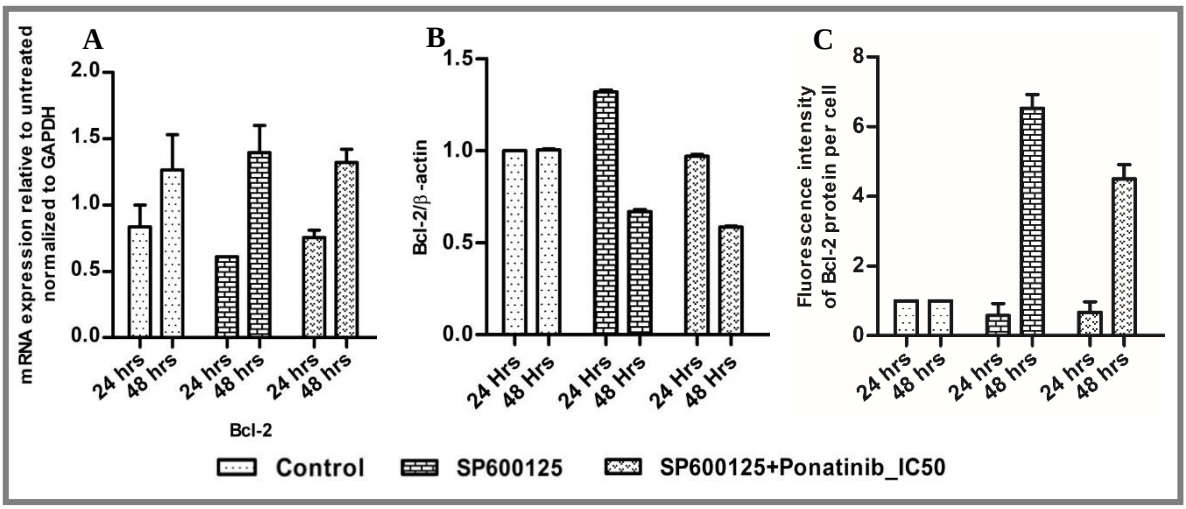

Figure 4.29. Influence of SP600125 with or without Ponatinib on Bcl-2 at mRNA and Protein Levels. This figure delves into the impact of SP600125, recognized as a cellular fate regulator that can effectively regulate autophagy and apoptosis, in the presence or absence of Ponatinib (PON) when applied at the IC50 concentration, specifically focusing on Bcl-2. The analysis encompasses both mRNA and protein levels. **(A)** The figure investigates the influence of SP600125 with or without Ponatinib (PON) on Bcl-2 mRNA expression. This analysis involves the measurement of normalized fold changes in Bcl-2 mRNA levels utilizing real-time quantitative PCR. The data undergoes double normalization, referencing both the control sample and the GAPDH gene, which serves as a loading control in the real-time q-PCR experiment. **(B)** The assessment continues with the determination of the relative density value of Bcl-2 protein using a western blot assay. The data is normalized to the control sample, with β-Actin employed as the loading control in the western blot assay. **(C)** To probe the effect of SP600125, with or without PON at the IC50 concentration, on Bcl-2 expression, the fluorescence intensity of Bcl-2 protein per cell was quantified via an immunofluorescence assay employing confocal microscopy. The data was subsequently normalized to the control sample. The experimental design includes observations conducted at both 24- and 48-hour intervals, enabling the examination of how Bcl-2 expression changes over time in response to the treatments. The symbols and bars featured in the figure represent the mean values along with the standard error of the mean (SEM), calculated from three independent experimental repetitions. Data analysis is conducted using GraphPad Prism and ImageJ software.

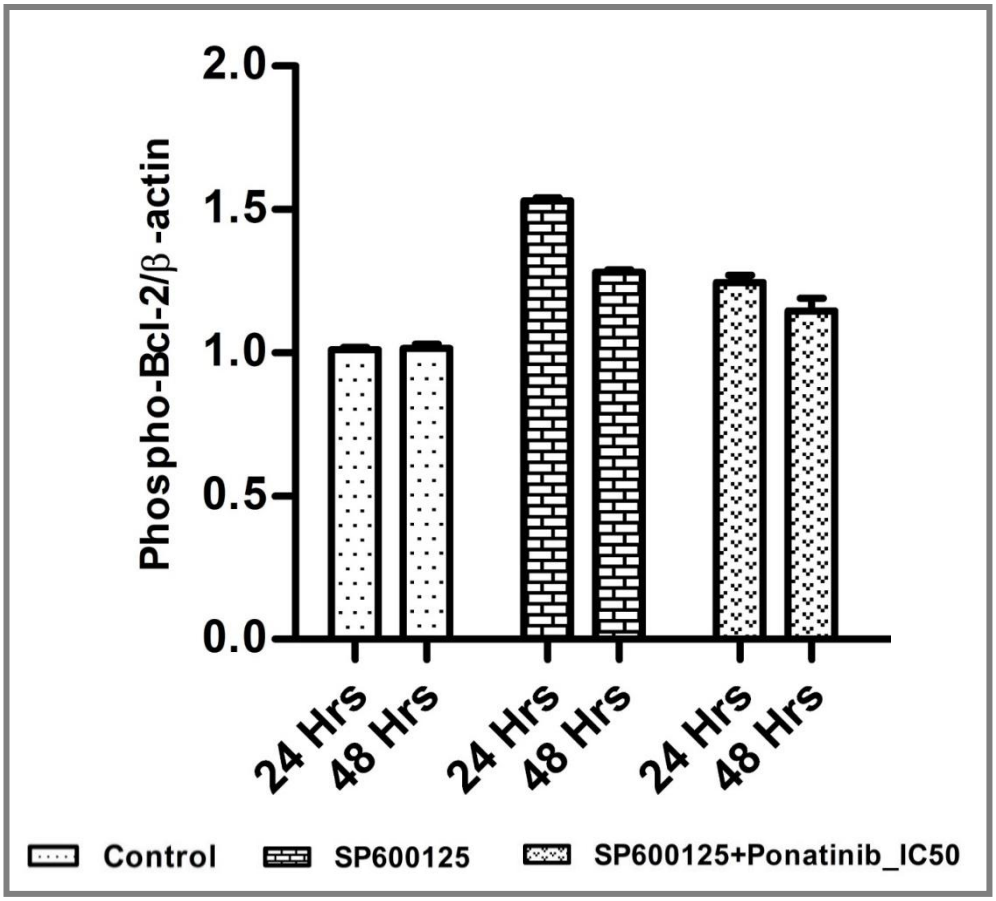

Figure 4.30. Influence of SP600125 with or without Ponatinib on Phospho-Bcl-2 Protein Levels. This figure is dedicated to understanding the influence of SP600125, a recognized cellular fate regulator capable of effectively regulating autophagy and apoptosis, in the presence or absence of Ponatinib (PON) when administered at the IC50 concentration. The focus here is on the levels of Phospho-Bcl-2, a crucial component within the regulatory pathways under scrutiny. Phospho-Bcl-2 Expression Analysis: The investigation involves a comprehensive assessment of the alterations in Phospho-Bcl-2 expression. This analysis is accomplished by quantifying the relative density value via western blot analysis. The collected data is scrupulously normalized to the control sample. β-Actin is the chosen loading control for the western blot assay. The experimental design encompasses distinct time intervals, specifically at 24 and 48 hours, providing a comprehensive view of changes over time in response to the treatments. The symbols and bars presented within the figure depict the mean values accompanied by the standard error of the mean (SEM), obtained from meticulous analysis involving three independent experimental replicates. Data analysis is executed with the aid of GraphPad Prism and ImageJ software.

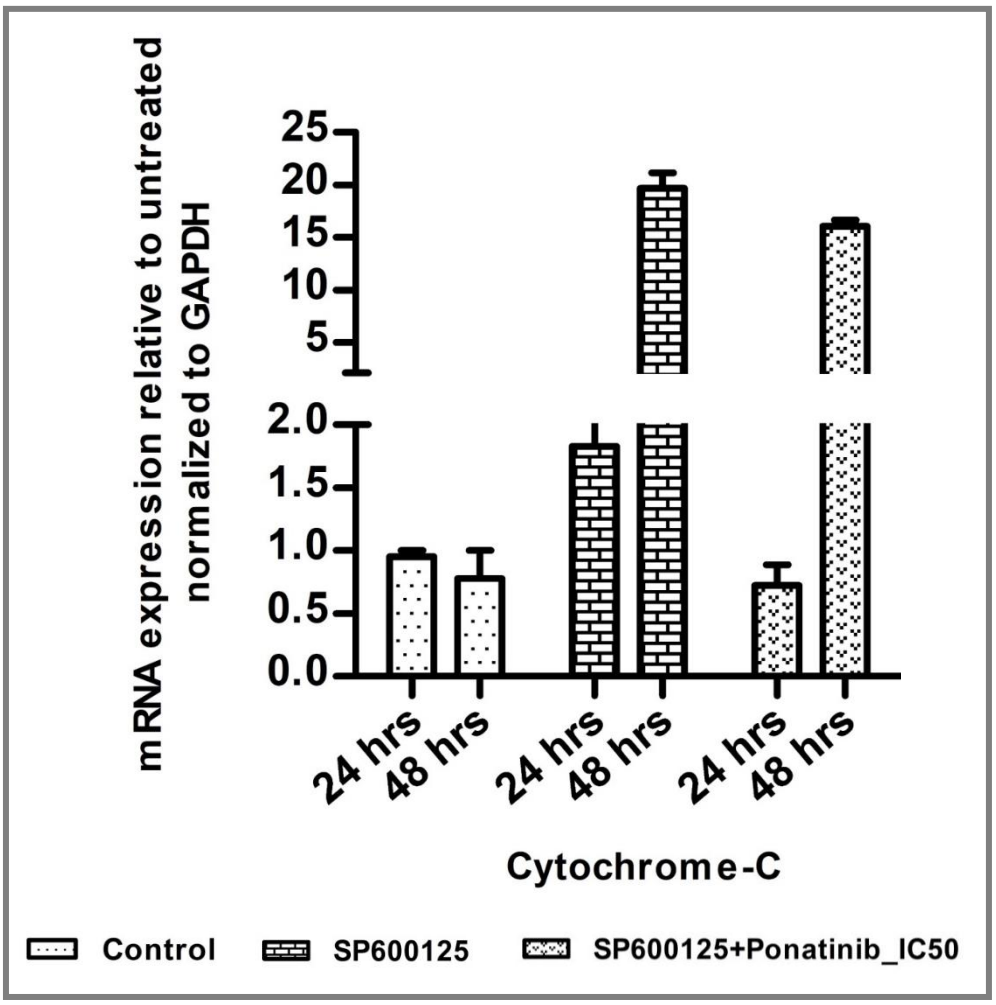

Figure 4.31. Influence of SP600125 with or without Ponatinib on Cytochrome-c at mRNA Level. In this figure, we explore the impact of SP600125, a recognized cellular fate regulator capable of effectively regulating autophagy and apoptosis, both in the presence and absence of Ponatinib (PON) at its IC50 concentration, on Cytochrome-c expression at the mRNA level. Cytochrome-c plays a pivotal role in the regulatory pathways under examination. The analysis involves the evaluation of changes in Cytochrome-c mRNA expression, conducted via real-time quantitative PCR. The data is subjected to double normalization, referencing both the control sample and the GAPDH gene, which serves as a loading control in the real-time q-PCR experiment. The experimental framework encompasses time intervals of 24 and 48 hours, providing insights into changes occurring over these durations. The symbols and bars featured in the figure represent the mean values along with the standard error of the mean (SEM). These results are derived from a robust analysis based on three independent experimental replicates. Data analysis has been diligently executed through the utilization of sophisticated software tools, including GraphPad Prism and ImageJ.

4.3.7 Ponatinib sensitizes the MCF-7 cells to autophagy-mediated cell death and showing pronounced effect with pharmacological modulators of autophagy and apoptosis.

Upon meticulous examination of the impact of the pharmaceutical compound ponatinib on the regulation of autophagy and apoptosis and its interaction with various pharmacological modulators at both RNA and protein levels, our study sought to corroborate the compound's tendency to promote autophagy-mediated cell death. This investigation was achieved through the Annexin-APC and 7-AAD-based apoptosis assay, utilizing a flow cytometer. It is essential to delineate the mechanistic aspects of apoptosis, wherein early apoptotic events are capable of reversible, leading to cellular survival. In contrast, the progression to late-stage apoptosis is characterized by an irrevocable fate. It is imperative to note that once autophagic cell death has been initiated and transitioned into apoptosis, any possibility of reverting to a state of survival is precluded. Hence, our focus was exclusively on the late apoptotic cell population throughout the experiments conducted in the context of the flow cytometry-based apoptosis assay. We scrutinized the influence of ponatinib in conjunction with various autophagy and apoptosis regulators at two distinct time points, precisely 24 hours and 48 hours. As established in the preceding section, our findings unveil an augmentation of autophagy-mediated cell death attributable to ponatinib over the 24 to 48-hour temporal progression. In the apoptosis assessment, it was discerned that upon exposure to ponatinib at its IC50 concentration (Figure 4.32), the late apoptotic population increased from ~12 % at 24 hours to ~17 % at 48 hours. A parallel effect was observed when cells were exposed to a 2IC50 concentration of ponatinib, resulting in a late apoptotic cell population of ~13 % at 24 hours, escalating to ~18 % at 48 hours. Consequently, our results suggest a time-dependent increase in the subpopulation of cells predisposed to irreversibility.

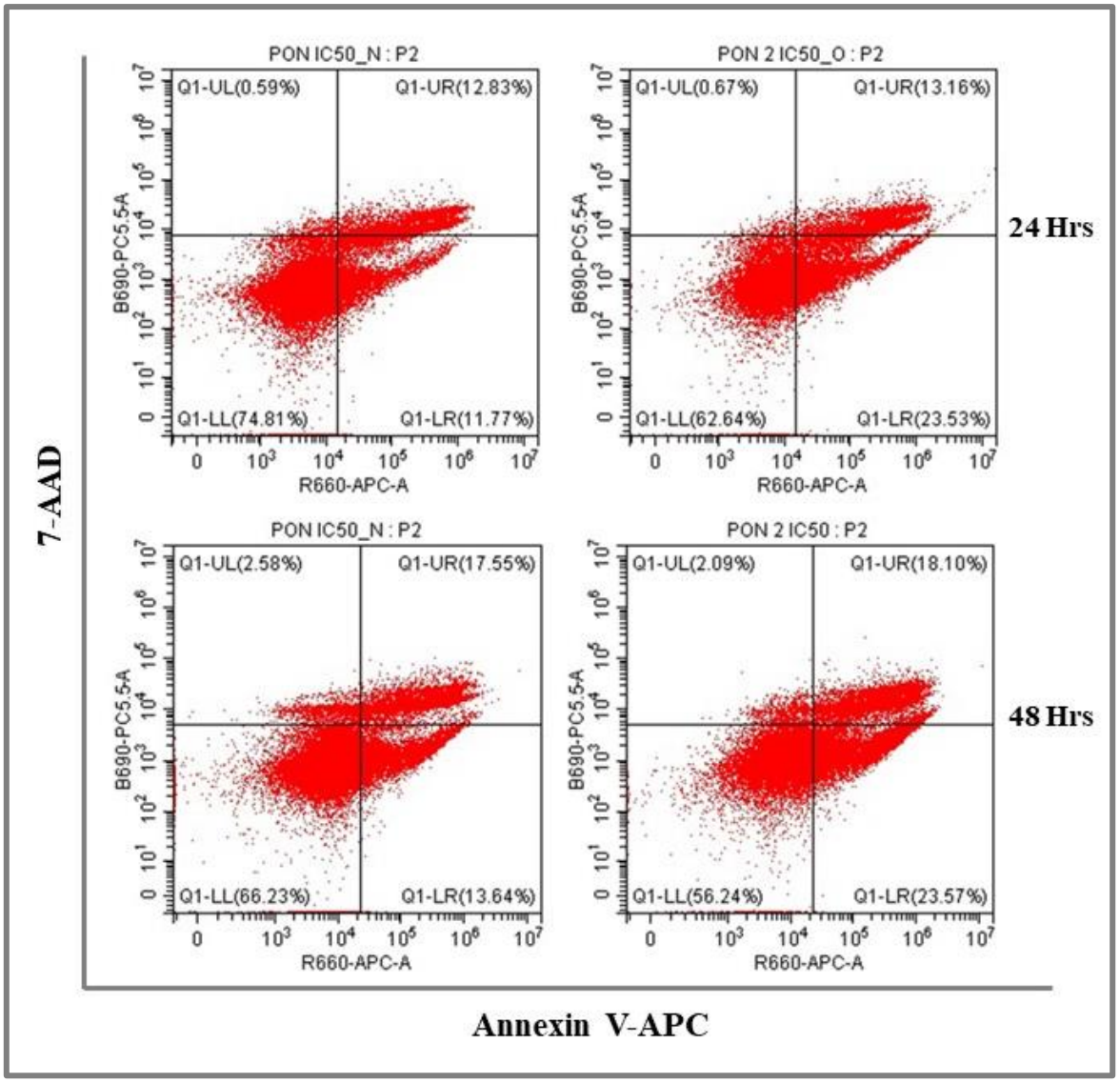

Figure 4.32. Apoptosis Assay for examining the apoptotic effect of PON. The apoptosis assay utilized flow cytometry to investigate the apoptotic response of cells following treatment with Ponatinib (PON) at concentrations corresponding to the IC50 and 2IC50 for 24- and 48-hour time points. The flow cytometry analysis enabled the assessment of apoptotic cells based on distinct criteria. Of particular significance is the cell population found in the upper right quadrant of the flow cytometry plot, which signifies late apoptotic cells. Notably, a compelling observation was made as the duration of treatment extended from 24 to 48 hours. This observation revealed a noticeable increase in the population of cells classified as late apoptotic in the upper right quadrant. This suggests a time-dependent elevation in the apoptotic cell population under the influence of Ponatinib. The data presented in this assay is representative of the findings from three independent experiments.

Furthermore, we explored whether rapamycin synergistically affected ponatinib's propensity for autophagy-mediated cell death (Figure 4.33). Intriguingly, at 24 hours, the late apoptotic population was noted at ~10 %, and this proportion increased to ~27 % as the observation period extended. In isolation, the administration of rapamycin yielded a late apoptotic population of ~6 % at 24 hours, which subsequently escalated to ~14 % at 48 hours. This compelling evidence indicates that rapamycin indeed augments the effects of ponatinib.

To ascertain that the late apoptosis induced by ponatinib is indeed autophagy-mediated, we employed 3-MA as a pharmacological agent to inhibit autophagy one hour before ponatinib exposure. Notably, the combined effect of 3-MA and ponatinib resulted in a decline of the late apoptotic population from ~16 % to ~7 % between the 24 and 48-hour time points (Figure 4.34), lending credence to the notion that late apoptotic events are an outcome of autophagy-mediated cell death.

Furthermore, we examined whether ponatinib induced independent apoptosis or if its actions were inherently linked to autophagy-mediated cell death. In this context, we employed the well-known apoptosis inducer, Doxorubicin (Figure 4.35). The combined effect of ponatinib and Doxorubicin demonstrated a late apoptotic cell population of ~36 % at 24 hours, compared to ~41 % observed with Doxorubicin alone. A similar pattern was evident at 48 hours, with the combined effect resulting in ~40 % late apoptotic cells, in contrast to Doxorubicin alone, which yielded ~43 % in the late apoptotic cell population. These observations substantiate the premise that ponatinib's action is not solely attributed to independent apoptosis mechanisms.

Subsequently, we undertook investigations to validate that the late apoptosis was not independently induced but rather an outcome of autophagy-mediated cell death. To this end, we employed SP600125, a compound known to inhibit independent apoptosis while promoting autophagy-mediated cell death. When combined with ponatinib, SP600125 demonstrated a notable induction of cell death, with the late apoptotic population increasing from ~9 % at 24 hours to ~12 % at 48 hours. However, it is essential to note that the combined effect of SP600125 and ponatinib did not display synergism when compared to the effect of SP600125 in isolation (Figure 4.36).

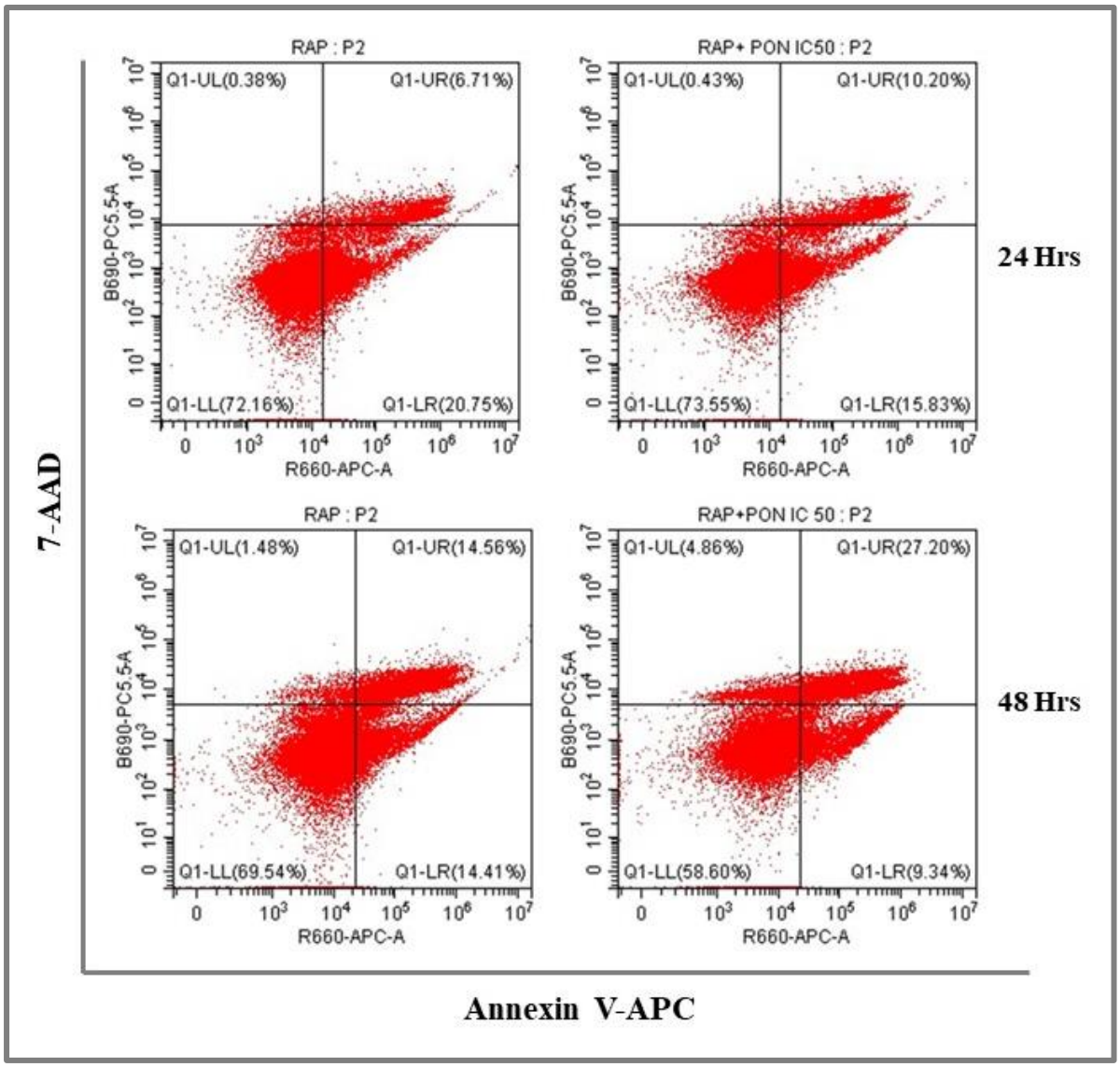

Figure 4.33. Apoptosis Assay for examining the apoptotic effect of Rapamycin (RAP) with and without the addition of Ponatinib (PON). The apoptosis assay utilized flow cytometry to investigate the apoptotic response of cells following treatment with RAP with and without the addition of PON at concentrations corresponding to the IC50 for 24- and 48-hour time points. The data presented in this assay is the best representative of the findings from three independent experiments.

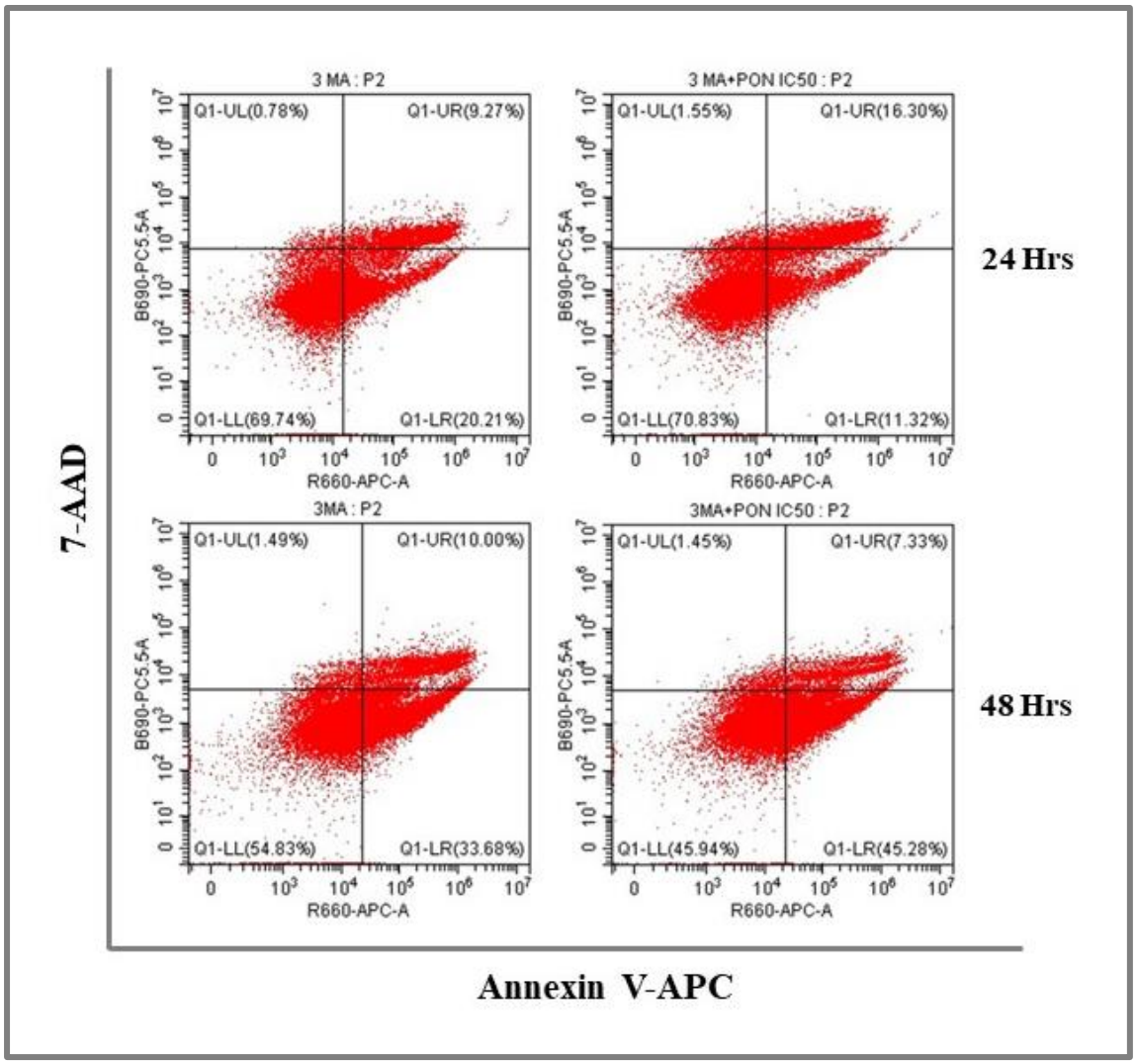

Figure 4.34. Apoptosis Assay for examining the apoptotic effect of 3-Methyladenine (3-MA) with and without the addition of Ponatinib (PON). The apoptosis assay utilized flow cytometry to investigate the apoptotic response of cells following treatment with 3-MA with and without the addition of PON at concentrations corresponding to the IC50 for 24- and 48-hour time points. The data presented in this assay is the best representative of the findings from three independent experiments.

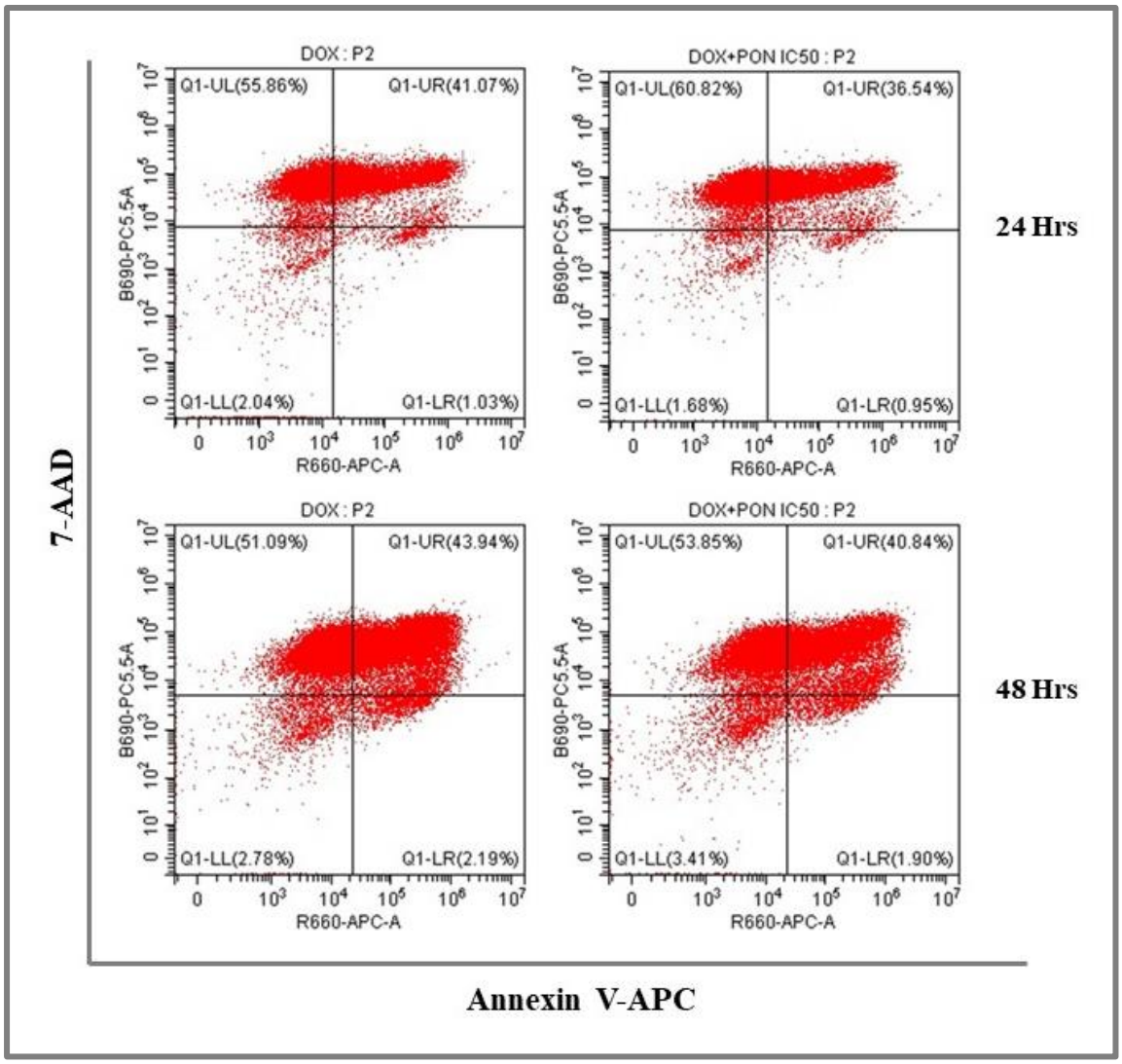

Figure 4.35. Apoptosis Assay for examining the apoptotic effect of Doxorubicin (Dox) with and without the addition of Ponatinib (PON). The apoptosis assay utilized flow cytometry to investigate the apoptotic response of cells following treatment with Dox with and without the addition of PON at concentrations corresponding to the IC50 for 24- and 48-hour time points. The data presented in this assay is the best representative of the findings from three independent experiments.

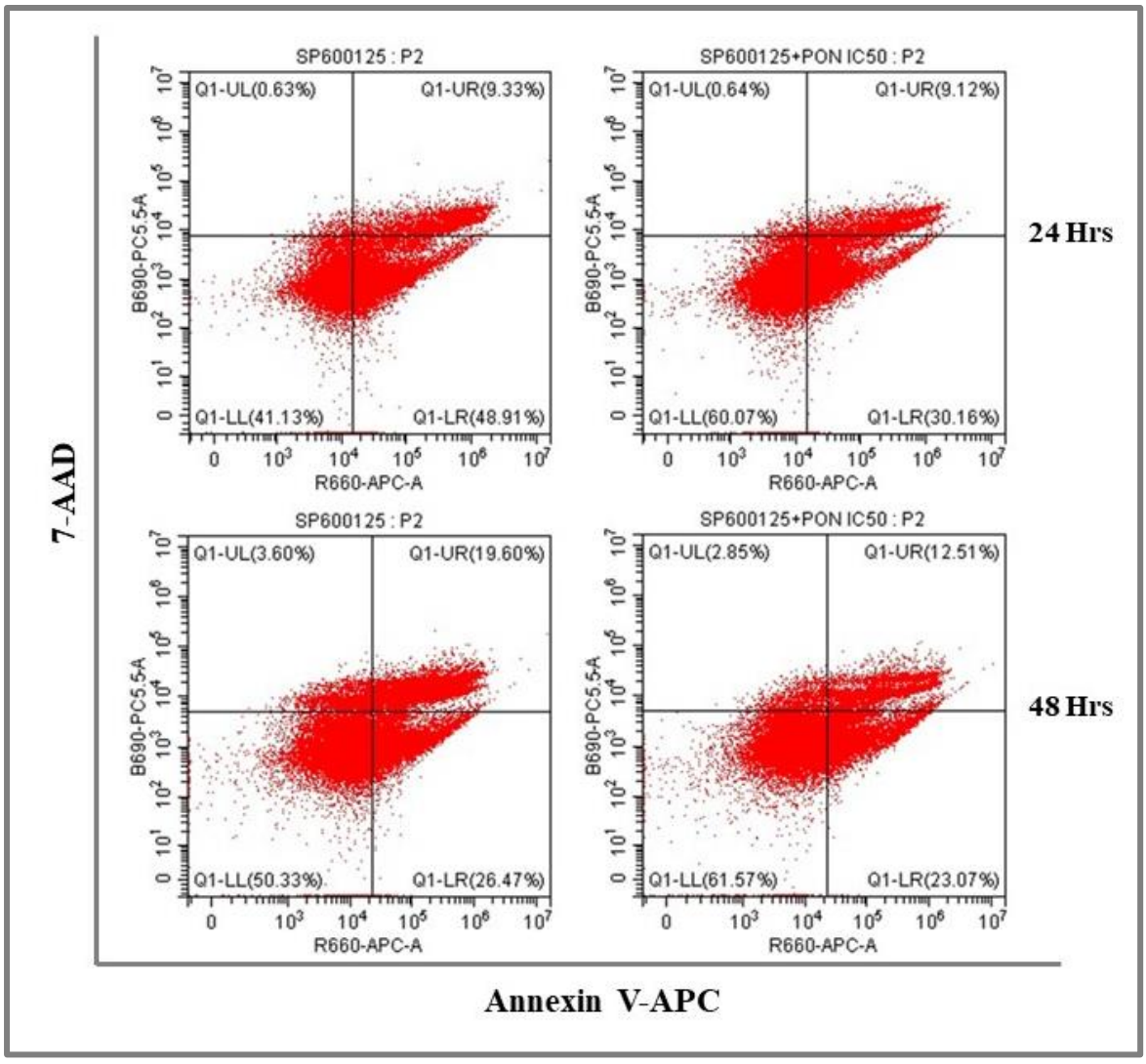

Figure 4.36. Apoptosis Assay for examining the apoptotic effect of SP600125 with and without the addition of Ponatinib (PON). The apoptosis assay utilized flow cytometry to investigate the apoptotic response of cells following treatment with SP600125 with and without the addition of PON at concentrations corresponding to the IC50 for 24- and 48-hour time points. The data presented in this assay is the best representative of the findings from three independent experiments.

Collectively, the outcomes of our experiments, spanning RNA and protein analyses as well as the apoptosis assay, consistently align with our working hypothesis. They substantiate the potent capacity of ponatinib to modulate autophagy and apoptosis by mediating the interaction between Beclin-1 and Bcl-2. This mediation involves the likely disruption of the Beclin-1-Bcl-2 interaction at the molecular interface, instigating a cascade of events. Initially, autophagy is upregulated within the cellular milieu, serving to meet heightened nutritional demands. However, as time progresses, a complex interplay of signaling mechanisms culminates in the inhibition of autophagic flux, rendering the tumor cells increasingly sensitive to apoptosis induction by ponatinib. This heightened propensity for autophagy-mediated cell death was validated through a repertoire of pharmacological agents capable of modulating autophagy and apoptosis pathways. Notably, our findings reveal that rapamycin, a potent autophagy regulator, synergistically amplifies the effects of ponatinib, underlining the multifaceted nature of these interactions. Additionally, the impact of 3-MA, an autophagy inhibitor, further substantiates that the late apoptotic events stem from autophagy-mediated processes. The concurrent use of Doxorubicin, an apoptosis inducer, underscores that ponatinib's actions do not manifest as independent apoptosis. Lastly, the amalgamation of SP600125 and ponatinib underscores that the observed late apoptosis is not an autonomous process but rather arises from autophagy-mediated cell death. To further elucidate the implications of these findings, *in vivo* studies can be warranted to gain a comprehensive understanding of ponatinib's role as an autophagy modulator and its potential applications in cancer therapeutics.

4.4 Conclusion

The well-established physiological roles of autophagy and apoptosis in processes such as development, aging, and normal cellular functions stand in stark contrast to the intricate interplay between these mechanisms in various pathophysiological contexts. These contexts include cancer, neurodegenerative disorders, cardiac abnormalities, bacterial and viral infections, and inflammatory diseases, constituting a complex and relatively underexplored phenomenon. The challenge in comprehending this interplay arises from its dynamic nature. In response to a stressed microenvironment, characterized by conditions like nutrient scarcity or therapeutic interventions, autophagy can exhibit a dual role, either supporting cell survival or promoting the progression of diseased states. Unlike apoptosis, autophagy showcases a context-dependent and stress threshold-dependent behavior.

While there is a burgeoning interest and recent initiatives to elucidate this intricate interplay, our understanding remains in its nascent stages, offering only partial insights into key regulators. Among these, Beclin-1 assumes particular significance. The autophagic protein Beclin1 demonstrates a stress-dependent ambivalence across various pathophysiological conditions. In the context of cancer, as cellular stress escalates, Beclin-1-mediated autophagy adopts a hierarchical profile, shifting from its role as a tumor suppressor to becoming a promoter of tumorigenesis. This transition is associated with chemotherapeutic resistance. Furthermore, there is emerging evidence supporting the potential of autophagy modulators as candidates for cancer therapeutics. Nevertheless, these insights necessitate further investigation to discern their applicability as targets within synergistic pathways for the development of innovative chemotherapeutic strategies.

The interaction between Beclin-1 and Bcl-2 is a pivotal regulatory axis in the orchestration of autophagy and apoptosis. Through prior in silico investigations, we endeavored to identify candidate drugs, such as Ponatinib, which exhibit strong binding

affinities with the BH3 domain of Beclin-1. We postulated that such drugs, upon binding, could disrupt the interaction between these two proteins, potentially serving as autophagy modulators. To validate the effect of Ponatinib on the interaction between Beclin-1 and Bcl-2, comprehensive *in vitro* experiments were conducted. Our selection of the breast cancer cell line MCF-7 for experimentation was motivated by the well-documented downregulation of autophagy in many breast cancer cells. Therefore, our aim was to investigate the impact of Ponatinib on the interaction between Beclin-1 and Bcl-2 in the context of breast cancer, with the objective of modulating autophagy and potentially driving the transition from autophagy to apoptosis.

This investigation yielded noteworthy findings: Ponatinib demonstrated the capacity to modulate autophagy, as indicated by alterations in Beclin-1 and Bcl-2 expression at both RNA and protein levels, and was further corroborated by cell viability assays. Additionally, Ponatinib exhibited the potential to induce apoptosis in breast cancer cells. Our data suggests that in addition to known mode of action of ponatinib as an anti-cancerous agent, this molecule appears to have the second mode of action through modulating autophagy-apoptosis cross-talk which is being reported for the first time. Furthermore, these results suggest that Ponatinib may mitigate its toxic effects through synergistic interactions with various autophagy modulators. This approach may diminish the impact of chemotherapeutic resistance and enhance tumor clearance, representing a promising avenue for therapeutic intervention in cancer treatment.